SIMBIO-M 2014, SIMulation technologies in the fields of BIO-Sciences and Multiphysics: BioMechanics, BioMaterials and BioMedicine, Marseille, France, june 2014

Michel Behr, Maxime Llari

SIMBIO-M 2014

INTERNATIONAL CONFERENCE
Marseille, France
June 19-20 2014

Faculté de Médecine
La Timone

Michel BEHR, Maxime LLARI (Eds)
Contact: simbio-m@ifsttar.fr
Web: simbio-m.ifsttar.fr

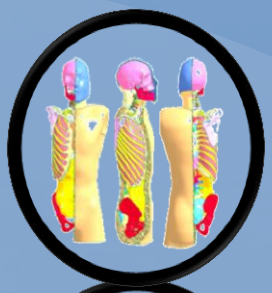

SIMulation technologies in the fields of **BIO**-Sciences and **M**ultiphysics: BioMechanics, BioMaterials and BioMedicine

Conference Chairmen

Kambiz KAYVANTASH - CADLM, FR
Pierre-Jean ARNOUX - IFSTTAR/AMU (LBA), FR
Christophe BASTIEN - Coventry University, UK

Organized by

CADLM · Coventry University · LBA · IFSTTAR · Aix*Marseille université

Sponsors

DASSAULT SYSTEMES · Altair · Technologies ALYOTECH

Eurobiomed Biocluster Méditerranée · European Society of Biomechanics

Conference Program

Welcome to the 2014 SimBio-M conference. The program of these two days will be as follows.

Thursday June 19th 2014

8:00 – 9:00	Registration
9:00	**Opening speech by Pr J.L. Mège** Medical Faculty Scientific Director of Aix-Marseille University **Welcome speech by the conference chairmen**
9:15	**Keynote lecture by Pr Clive Neal-Sturgess** Emeritus Professor of Mechanical Engineering The University of Birmingham Visiting Professor of Clinical Biomechanics Birmingham City University Visiting Professor of Automotive Safety Coventry University Injury Causation – Peak Virtual Power

Session 1 – Biomedical applications I Chairman: K. Kayvantash

10:00	**B. Baillargeon** - A Proof-Of-Concept simulator for human heart function
	B.L. Davis - Simulating knee reconstruction surgery: relationships between joint surfaces and ligament placement
	R. Bianco - Biomechanical study of surgical parameters on pedicle screw pullout strength
10:50	Coffee break

Session 2 – Biomedical applications II Chairman: C. Neal-Sturgess

11:10	**S. Tusch** – Multicomponent vesicles in wall bounded shear flow
	M. Avalle - Topological Optimization of Denthal Prostheses
	P Hebert - Micromechanical modelling for wood-fiber reinforced plastics

Session 3 – Biomaterials Chairman: M. Avalle

12:00	**A. Garo** - Evaluation of Humos II for side facing aircraft seat application
	L. Fradet - Finite element study of cervical spinal dislocation with spinal cord injury: preliminary results
	A. Naaim - Correcting soft tissue artefact through multi body-optimization: Proposition of an anatomical upper limb kinematic model
13:00 – 14:00	Lunch

Session 4 – Imaging tools I Chairman: C. Bastien

14:00	**M. Julias** - A Meta-Analysis on Biological Variation in Simulations: Importance and Current Modeling Practices
	M. Taso - From Spinal Cord MRI to a realistic 3D FE model of the spine and spinal cord
	R. Perz - Two-Dimensional Digital Image Correlation (DIC) Efficacy Assessment for Strain Measurement on Bone Surface

Session 5 - Imaging tools II Chairman: K. Chaumoitre

14:50	**M. Pedzisz** - Global and local personalization of a complicated human body FE model.
	A.S. Studer - Towards splenic modelling: what is the impact of spleen anatomy on injury severity in blunt splenic trauma?
	J. Brunet - Elastography: from traumatology to the evaluation of preterm labor risk
	S. Coze - Blunt hepatic trauma: Influence of liver morphology in patients evaluated with volumic CT scan
15:40 – 16:00	Coffee break

Biorezo session -
in association with EUROBIOMED

16:00	**S. Monneret** - Lighting the living **P. Spiga** - Interdisciplinary approach for medical imaging **B. Loubaton** – Renewal of molecular imaging : The ISI LOTUS Project
17:30 – 18:00	Round Table
18:00	Cocktail

20:30	Gala Dinner http://www.rowing-clubrestaurant.com/

Friday June 20th 2014

9:00	P. Guilhou - Presentation from DASSAULT SYSTEMES

Session 6 – Road Safety *Chairman: C. Kahn*

9:20	**D. Montoya** - Influence of car design in typical child pedestrian accident : a parametric study
	J. Vychytil - Scaled model for pedestrian safety
	H. Hamdane - Assessment methodology of Active Pedestrian Safety Systems: an estimation of safety impact.
	F. Auriault - Predicting adverse fetal outcomes in road accidents
	C. Bastien - Suitability of a Multi-Body based Active Human Model for Kinematics and Injuries simulations in an Automatic Emergency Braking Scenario
10:55 – 11:10	Coffee break

Session 7 – Outdoor activities *Chairman: L. Hyncik*

11:10	**M Behr** - Outsole material and architecture optimization to reduce lower limbs exposure during typical soccer movements
	S. Li - Modeling Simulation on Horse-Jockey System
	N. Bailly - Parametric study of a snowboarding accident: Implication on helmet standard
12:00 – 13:15	Lunch

Session 8 – Biomaterials: human tissue *Chairman: Y. Tillier*

13:15	**C. Savoldelli** - A finite element study of the effects of distraction osteogenesis on the temporomandibular joint
	A. Roux - Tensile response of muscle-tendon complex using discrete element modeling
	L. Ren - Investigation of diffuse axonal injury mechanism and thresholds via the combination of finite element simulation and in vivo experiment
	F. Lanzl - Superficial soft tissue modelling in impact loading
	G. Tod - An upper limb musculoskeletal model using bond graphs for rotorcraft-pilot couplings analysis
14:45 – 15:00	Coffee break
15:00 – 15:30	Word from our Award Sponsor (H. Shakourzadeh, ALTAIR) Awards distribution Closing words by the Chairmen

A Proof-Of-Concept simulator for human heart function

Brian Baillargeon[1], Ellen Kuhl[2], Michèle Alexandre[3(*)]

[1] *Dassault Systèmes Simulia Corporation, Fremont, CA 94538, USA*

[2] *Dep. of Mechanical Engineering, Bioengineering, and Cardiothoracic Surgery, Stanford University, Stanford, CA 94305, USA*

[3] *Dassault Systèmes SA, 78140 Vélizy-Villacoublay, FRANCE*

Keywords*:* cardiac mechanics; electro-mechanics; excitation-contraction; finite element analysis

1. Introduction

The heart is one of the most complex organs, controlled by the interplay of electrical and mechanical fields. It consists of four chambers and four valves which act in concert to produce an overall pump function. But the integrative electro-mechanical response of the whole heart remains poorly understood. Here we present a proof-of-concept integrative simulator developed in the Finite Element environment of Abaqus [1]. The model supports the excitation-contraction coupling, as well as a simplified approach of the fluid-structure interaction. Electrical potential and mechanical deformation are visualized across the human heart throughout a cardiac cycle. The pressure - volume relationship, as well as the apex movement compared against common metrics of cardiac function agrees well with clinical observations.

2. Methods

The four-chamber human heart model was created from computer topography and magnetic resonance images [2]. The initial geometry was subsequently modified to make it more suitable for meshing with tetrahedral elements.

The electro-mechanical coupling developed in [3] assumes that the tissue stress consists of passive and active contributions. The active stress developed in the cardiac muscle fiber direction and in the sheet direction is a time varying excitation, which depends on the electrical potential.

The transient electrical response is characterized by an action potential ϕ and a recovery variable r. Both isotropic and anisotropic contributions are considered to account for faster conductivity along the fiber direction.

The blood flow model consists of a combination of surface-based fluid cavities and fluid exchanges based on viscous resistance.

The analysis workflow currently uses a sequentially coupled analysis approach, where the electrical analysis is run first, and then the electrical potentials are mapped onto the mechanical analysis as the excitation source.

3. Results and Discussion

The FE model is composed of 208562 linear tetrahedral elements and 47323 nodes.

The simulation represents a cardiac cycle over 600ms. The model provides the electrical potential and deformation as a function of time throughout the solid model.

Other typical results are measurement of the apex displacements and pressure-volume loops for the four chambers. The apical lift is about 7.0mm and agrees with published clinical or simulation data [4].In spite of our simplified fluid flow model, the pressure-volume loop recorded with the left ventricular fits within clinically expected range.

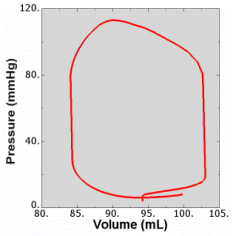

4. Conclusions

This proof-of-concept simulator provides the basis of a whole heart model able to represent the heart dynamics. This model still has a few limitations, which can be addressed with modular changes and minor refinements. But the ultimate goal is to utilize this simulator to investigate heart behaviour, device design and treatment planning in the numerous cardiac diseases.

References

[1]Abaqus 6.13 Analysis User's Manual. Simulia. Dassault Systèmes

[2] Zygote Media Group, Inc., 2013. The Zygote Solid 3D Heart Model.

[3]Baillargeon B., Rebelo N., Fox D.D, Taylor R.L, Kuhl E., 2014. The living Heart Project: A robust and integrative simulator for human heart function. *Preprint submitted to European Journal of Mechanics and Solids*

[4]Wong J., Göktepe S., Kuhl E., 2013. Computational modeling of chemo – electro - mechanical coupling: A novel implicit monolithic finite approach. *Int. J. Num. Meth. Biomed. Eng.*

***Corresponding author. Email: michele.alexandre@3ds.com**

Simulating knee reconstruction surgery: relationships between joint surfaces and ligament placement

Brian L. Davis[1], Melissa A. Boswell, Calia Battista

[1]*Department of Biomedical Engineering, The University of Akron, OH 44325* http://bme.uakron.edu

Keywords*:* knee, kinematics, ligaments, biomechanics, orthopedics

1. Introduction

Patients have knees with varying geometry. The shapes of their cartilage surfaces have a profound effect on the kinematics of the femur relative to the tibia. Despite this, every patient who has knee reconstruction, has the ligament placed in a standard location. While this may work for a subset of the population, there are post-surgery patients with ligaments that are either too tight or too lax following the reconstruction procedure. This study focused on the degree to which curvatures of the femur affected the required lengths and placement of reconstructed knee ligaments.

2. Methods

An initial knee model was created using Solidworks CAD software. Lengths and attachment points Bradley et al. (1998) of the ACL and PCL were used to create a four bar linkage. Radii of the medial and lateral femoral condyles (Siu et al. 1996) were used to create arcs in parallel sagittal planes. The orientation of the condylar arcs and the four-bar linkage was determined using sagittal MRI image data (Csillag, 1999). A reference point on the patellar ligament was taken along the same horizontal plane as the tibial plateau. The distance was found between the point and insertion of the PCL on to the tibia, and the four-bar linkage was oriented during standing as found in the image. Finally, the condyles were arranged so that the tangent of the two radii of the lateral condyle were closest to the tibia during the 'screw home' mechanism that occurs starting at 30 degrees from full extension (McGinty, Irrgang, Pezzulo, 2000).

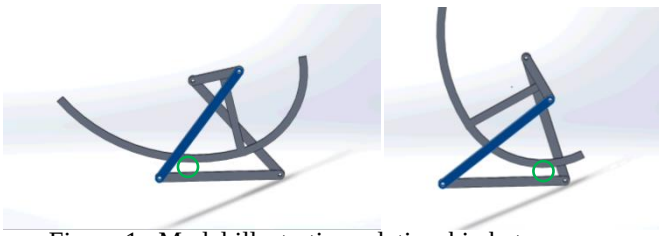

Figure 1. Model illustrating relationship between condyle radii and ligament lengths: (left) knee in extended position, (right) knee in flexed orientation. Note the gap between femur and tibia (green circles) is constant in this model, indicating compatibility between ligament and joint surfaces.

Figure 2. Model with same femoral radii as before, but sub-optimal ligament placement. In flexion, the femur is compressed into the tibia (red circle).

3. Results and Discussion

The simplified sagittal plane model of a knee showed mutual dependencies between ligament lengths (and positions) and the radii of curvature of the femoral condyles. Changing the lengths of a ligament by as little as 2mm in the model caused significant differences in the gap between the femoral and tibial articular surfaces.

4. Conclusions.

Physiological motion between femoral and tibial articular surfaces is only possible if the femoral condyle radii and knee ligament placements are compatible with each other. Studying these relationships offers insight into knee biomechanics that can benefit designers of knee implants and surgeons who reconstruct knees.

References

Bradley J, FitzPatrick D, Daniel D, Shercliff T, O'Connor J. (1998). Orientation of the Cruciate Ligament in the Sagittal Plane: A Method of Predicting its Length Change with Flexion. J Bone Joint Surg [Br]. (70-B): 94-99

Csillag, A. (1999). Anatomy of the Living Human : Atlas of Medical Imaging, Konemann Verlagsgessellschaft mbH, Koln. pp. 380-383.

McGinty G, Irrgang JJ, Pezzulo D. (2000). Biomechanical considerations for rehabilitation of the knee. Clinical Biomechanics. 15, 160-166.

Siu D, Rudan J, Wevers HW, Griffiths P. (1996). Femoral Articular Shape and Geometry: A Three-dimensional Computerized Analysis of the Knee. The Journal of Arthroplasty. 11(2): 166-173).

***Corresponding author. Email: bdavis3@uakron.edu**

Biomechanical study of surgical parameters on pedicle screw pullout strength

R-J. Bianco [1, 2, 3(*)], P-J. Arnoux [3], J-M. Mac-Thiong [2], E. Wagnac [1,3] and C-É. Aubin [1,2]

[1] *École Polytechnique de Montréal, Canada*

[2] *CHU Sainte-Justine, Montréal, Canada*

[3] *Laboratoire de Biomécanique Appliquée, Marseille, France*

Keywords*:* Finite Element Analysis; Pedicle Screw; Pullout.

1. Introduction

Pedicle screw-based internal fixation systems are widely used to correct severe spinal deformities and stabilize spinal segment. The screw has to remain well anchored in the vertebra during manoeuvres in order to withstand intra and post-operative functional loading. The screw choice and its placement have been shown to have an impact on the screw performance. There is no consensus among clinicians about an optimal screw geometry, size and placement. *In vitro* experiments provide insight into the biomechanics of screw-bone interactions, but show inherent limitations. The objective of this study was to computationally assess the effects of surgical parameters on the screw pullout strength.

2. Methods

A detailed FEM of a L3 vertebra was created from CT-scan images. The vertebra was modeled by taking into account the separation of the trabecular core and the cortical external layer with realistic regional thickness. It was meshed with tetrahedral elements of 0.4 mm characteristic length. The model integrates an elastoplastic material law (Johnson-Cook) with bone failure represented by element removal. Bone was considered as a homogeneous isotropic material. The screws were placed following anatomical landmarks and a contact interface contact was implemented between the bone and screw elements. The model was applied boundary conditions and loadings in order to simulate pullout tests as described in ASTM-F543 standard. The anterior part of the vertebral body was clamped and a tensile force was applied on the screw until it pulled out. A design of experiment of 4 screw factors (thread type, diameter, length and trajectory) was performed to study their effects on its biomechanical anchorage (initial stiffness and peak pullout force).

3. Results and Discussion

The model was validated by comparison of the obtained data with published experimental data. The design of experiment analysis showed that the diameter had the greatest impact on the screw anchorage (initial stiffness and peak pullout force). The screw length had a lower impact but still a significant effect ($p<0.01$). Those results suggest that the screw size choice had significant effect on its anchorage and physicians should always choose the largest and longest screw as anatomically possible. The results also showed that the best anchorage was obtained when the screw was placed close to the lateral cortical wall. A combined study of the design of experiment results and internal stress distribution in the bone structure showed that the single threaded screws have a better biomechanical anchorage than the dual treaded screws.

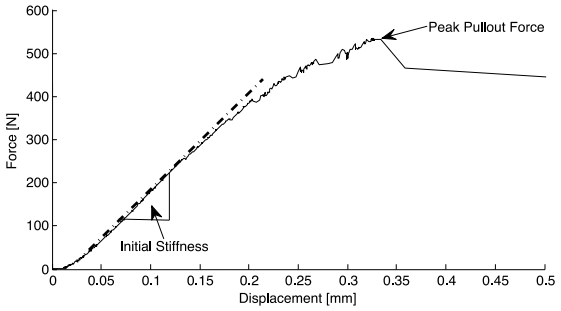

Figure 1: Force-displacement behavior of pullout screws and indices extracted

4. Conclusions

This detailed finite element model allowed to identify the pullout mechanism under axial loading and explain the effects of thread geometry on the behaviour of the bone structure. This model is a promising complementary tool to *in vitro* experimental tests. The perspectives are to use this tool as a testing platform for new implant designs or as a surgery-planning tool to help clinicians.

Acknowledgments

Funded by NSERC (NSERC/Medtronic Industrial Research Chair in Spine Biomechanics)

***Corresponding author. Email: rohan.bianco@gmail.com**

MULTICOMPONENT VESICLES IN WALL BOUNDED SHEAR FLOW

Simon Tusch[1], Kamel Khelloufi[1], Al-hair Al-Halifa[1], Marc Leonetti[2] & Annie Viallat[*]
[1]*Aix Marseille Université, CNRS LAI, UMR7333, Inserm UMR1067, 13009 Marseille, France*
[21]*Aix Marseille Université, CNRS IRPHE, UMR7342, 13384 Marseille, France*
[*]*Email: annie.viallat@inserm.fr*

Keywords: GUVs, bending energy, shape memory, tanktreading, tumbling

INTRODUCTION

Multicomponent vesicles have a lipid bilayer membrane containing two types of lipids and cholesterol. Below a critical temperature, multicomponent lipid vesicles exhibit phase separation of coexisting liquid phases and can present two separated domains with different spontaneous curvatures. The membrane therefore presents two types of elements that are not equivalent. We address the question of the dynamics of these two-domains vesicles under a shear flow, and more precisely to the regimes of tanktreading and tumbling.
In order to precise which specific questions arise on the dynamics of two-domains vesicles, it is necessary to recall the findings on homogenous vesicles and on red blood cells. Homogeneous vesicles present two main regimes of motion, tumbling and tanktreading, which depend on the viscosity ratio between the internal fluid and the suspending fluid and on the aspect ration of the vesicles. The red blood cells dynamics exhibits specific features: a swinging motion superimposed to the tanktreading motion, a chaotic regime in sinusoidal shear flow and a tanktreading-tumbling transition that depends not only on the viscosity ratio but also on the shear rate. These features are due to the shear elasticity of the cell membrane and to the fact that the membrane elements of the cell are not equivalent. Indeed, when the membrane elements located at the rim of the cell are displaced during tanktreading and reach the dimple of the cell, the shear elastic energy of the membrane increases because the membrane elements are strained with respect to the initial position (at the rim). It is the same for the elements initially located at the dimple that reach the rim. If the stress stops, the membrane elements go back to their initial position to minimize shear elasticity and this behavior is known as 'the shape memory of red blood cells'. When the shear rate is low, the hydrodynamic energy provided by the flow is less than the shear elastic energy required to strain sufficiently the membrane elements to allow their displacement from the rim to the dimple and vice-versa. Tanktreading is then impossible and the cell tumbles. Tanktreading occurs above the critical shear rate, that overcomes the barrier of strain energy of the membrane elements. This behavior does not exist for homogeneous vesicles for which all membrane elements are equivalent. Two-domains vesicles have in common with red blood cells to have a shape memory, but it is based on bending energy and not on shear elasticity like for red cells. Therefore, is the dynamics of two-domains vesicles similar to that of red blood cells?

METHODS

Lipids
We used a 4:4:2 (DOPC:DPPC:Cholesterol) mixture to prepare giant lipid vesicles. A percentage of 5 to 10% of fluorescent N-(lyssamine rhodamine B sulphonyl)-dipalmitoylphosphatidylethanolamine was added to visualize one of the two domains of the membrane.

Vesicle preparation
The vesicles were prepared by a standard electroformation method performed at 60°C. They were prepared in a sucrose solution at 100 mOsm

Flow experiments
Vesicles were diluted in a glucose solution at osmolarities varying from 100 mOsm to 160 mOsm to deflate the vesicles. They were introduced at room temperature in a 4-optical faces flow chamber (1mm height, 1 cm wide) placed on an inverted microscope (LEICA DMIRB, x20) tilted horizontally.

The flow was applied by using a syringe pump. Fluorescence microscopy and phase contrast microscopy were used to visualize the vesicles and their domains. Vesicle motion was recorded by a ANDOR Neo sCMOS camera.

RESULTS

A typical image of a resting vesicle is shown in figure 1A. A tanktreading vesicle is shown in figure 1B

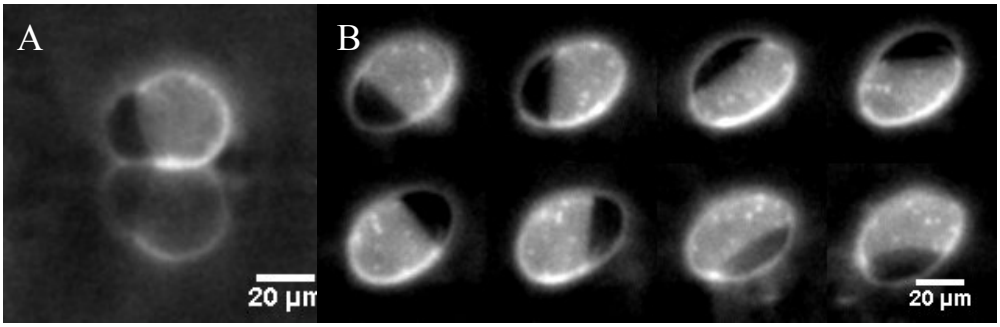

Figure 1 two-domains vesicle A: at rest; B: tanktreading two-domains vesicle in a shear flow, shear rate: $5s^{-1}$

We examine the motion of two-domains vesicles in shear flow as a function of the vesicle size, deflation ratio and shear rate. We determine the time variation of the angle between the long principal axis of the vesicle with respect to the flow direction is illustrated in Figure 1C and the position of the DOPC domain (fluorescent). We show that, similarly to the motion of red blood cells, the vesicle inclination was oscillating during tanktreading (swinging regime) and that the position of the DOPC domain at the pole or the equator of the membrane was directly correlated with the vesicle inclination (see figure 2) and we discuss the observed results.

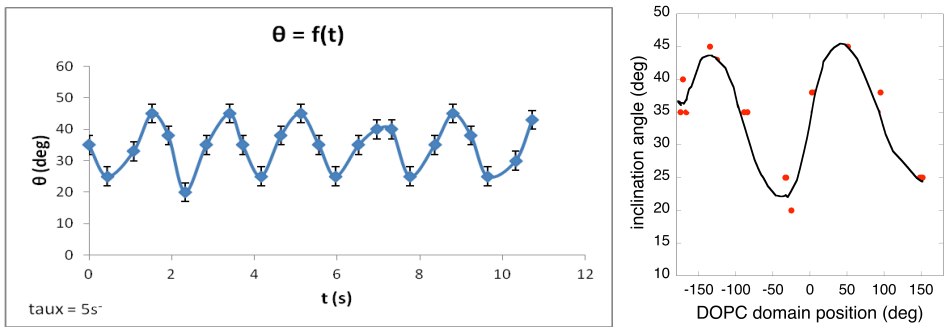

Figure 2. Left: Time variation of the vesicle inclination during tanktreading; right: correlation between the inclination angle and the position of the DOPC domain.

We also discuss the conditions for the tumbling motion and the effect of deflation on the regimes of motion. Finally we compare the motion of these vesicles to both that of homogeneous vesicles and that of vesicles displaying a large number of small domains that can be also observed for some vesilces

CONCLUDING REMARKS

We show that the dynamics of two-domains vesicles share very specific regimes of motion with red blood cells. However, shear elasticity plays a major role for red blood cells motion whereas it is the bending energy that plays a similar role for two-domains vesicles.

Topological Optimization of Denthal Prostheses

M. Avalle[1], A. Scattina[1] and P.C. Priarone[2]

[1] *Politecnico di Torino, Department of Mechanical and Aerospace Engineering*
Alessandria Technological Pole, Viale Teresa Michel 5, 15121 Alessandria, Italy

[2] *Politecnico di Torino, Department of Management and Production Engineering*
Corso Duca degli Abruzzi 24, 10129 Torino, Italy

Keywords*:* topological optimization; dental prostheses

1. Introduction

Dental prostheses are made of various types of bio-compatible materials, mainly metals but also, recently, plastics and composites. Attempts are continuously made in order to reduce the volume of the prosthesis and, consequently, the weight and cost while maintaining the necessary strength, endurance and stiffness. This in turn also strongly reliefs the patient pain and discomfort.
Aim of this work was to apply the topological optimization method to a dental prosthesis in order to minimize the weight by removing the unused material.

2. Methods

The topological optimization is a very effective method to find improved structural solutions in cases where complex and very ineffective geometries allow for dramatic interventions to remove unexploited material. Iteratively the algorithm works on the local material density to come to the optimized outcome.
The application of the method required a series of steps: first the mandibular geometry must be obtained, from CT scans or other techniques; then the volume of a basic dental prosthesis has to be designed and divided in design space, subject to optimization, and non-design space; finally, the loads coming from mastication must be applied. This is the most difficult problem due to the relatively unknown values and their variability: moreover, finding optimized solution for a load case leaves weaknesses to any other possible load variations.

3. Results and discussion

The topological optimization was applied to a *Toronto* bridge which is used as a structural support for the installation of the artificial teeth. The bridge is installed by means of implants.
After finding the best way to consider the boundary constraints, especially the mastication loads, an optimized prosthesis able to ensure a volume reduction of 60%, with displacements that do not disturb the patient during normal mastication, was obtained. Some first prototypes were built and are subject to testing with positive results.

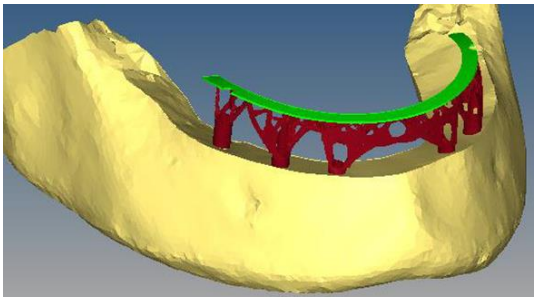

Figure 1 Result of the topological optimization of a *Toronto* bridge.

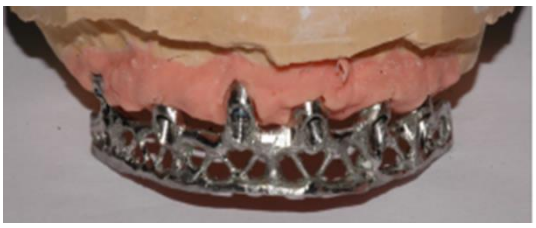

Figure 2 Optimized *Toronto* bridge prototype.

4. Conclusions

The topological optimization proved to be a valuable tool to help reducing the weight of a *Toronto* bridge while maintaining adequate structural characteristics. The main problem in the application of the method to this problem, relates to the definition of the proper boundary conditions. While this problem solved and the method applied, feasible solutions are obtained and can be easily transferred to manufacturing to obtain a very effective solution especially in case of critical patients where massive intervention are required.

Acknowledgments

The support of *Beldent Group* in the development of the work is gratefully acknowledged.

References

Shillingburg, Herbert T. Shillingburg. Fundamentals of Fixed Prosthodontics, 3rd Edition. Quintessence, 1997.

***Corresponding author. Email: massimiliano.avalle@polito**

Micromechanical modelling for wood-fiber reinforced plastics

Hebert Philippe and Toth Mira[1]

[1] *e-Xstream engineering SA, B-1435 Mont-Saint-Guibert, Belgium*

Keywords*:* Wood fiber

Wood fiber offers an alternative to glass fiber as reinforcement for injection molded thermoplastics. The lengthiameter ratio for a typical thermomechanical wood pulp is sufficiently large, even after the fiber-shortening effects of extrusion blending and injection molding, for the fibres to become partly oriented during flow through the mold. Optical microscopy of the cut surfaces of composites has shown that the morphology of wood fibers deviates from the rod-like shape of glass fibers, but that the degree of flow alignment is similar. Commercial software was used for micromechanical modelling of polypropylene reinforced with wood fibers. The results showed good matches between theoretical and experimental stress-strain curves, including good prediction of the consequences of differences in flow alignment between different locations in molded specimens, providing a clearer picture of the consequences of using wood fiber instead of glass fiber as reinforcement.

***Corresponding author. Email: Philippe.Hebert@e-xstream.com**

Evaluation of Humos II for side facing aircraft seat application

A. Garo[1] and F. Njilie [1]

[1] *Altair Development France, 5 rue de la Renaissance, 92160 Antony, France*

Keywords*:* side-facing seat, Humos II, aerospace, RADIOSS, crash

1. Introduction

The Federal Aviation Administration (FAA) has defined the requirements for aircraft seat certification concerning the emergency landing dynamic conditions for different categories of airplanes and rotorcrafts. This regulation is primarily focused on backward and forward facing seats.

In order to make the certification tests, the aircraft manufacturers use Anthropomorphic Test Devices (ATD), representative of the human body. Numerical modelling tools such as finite elements models are now used to facilitate the evaluation of aircrafts seating systems (AC 20-146 2003). In that case, numerical ATD are used. However, they are not as biofidelic as human numerical model. The benefits of human body models in term of realistic behavior, injuries prediction or specific organs studies are important.

In 2006, the European Commission, with many partners from the automotive industry, sponsored the creation of the Human Model for Safety 2 (HUMOS 2), a human finite element model. This model has been then adapted to be used in aircraft crash scenario (Njilie 2012), leading to the HUMOS2 AERO model. It has been validated in FAA fontal and vertical load cases conditions.

However, in the field of business jets, side-facing seats are quite popular. The risk of injury is totally different between side facing and forward facing seats (Philippens 2011). As a consequence, there is need to understand more precisely the human behavior in these specific conditions of impact during survivable emergency landing.

The purpose of this study was to adapt and improve the HUMOS2 AERO model to side facing tests conditions and to investigate the injury mechanism. The other objective was to compare the response of the human model to the ES2-re model, a side impact ATD.

2. Methods

HUMOS2 AERO model had the same instrumentation as the HUMOS2 model: it was equipped with channels to measure accelerations, elongations, forces and moments.

The HUMOS 2 AERO model was updated to be capable of providing the risk of injury in side impact loadings. The pubic load was defined as the normal force of a section defined in the pelvis cartilage. Ten springs without stiffness were created inside the ribcage in order to evaluate the ribs deflection in side impact loading.

Two configurations of tests, representative of typical aircraft side facing seat scenarios, were investigated (DeWeese 2007). In the first configuration, the occupant was placed next to a rigid wall. In the second configuration, the occupant was placed next to an arm-rest (Fig 1). A three-point system made of a lap belt and a shoulder belt was used as a restraint system. The seat was covered with foam cushion. A deceleration pulse of 16G, as defined in 14 CFR 25.562, was used.

The kinematics of the model and the risk of injury were investigated. Bones breaking was monitored by observing elements Von Mises stress reaching their maximal value.

The accelerations of the head, the pelvis, the upper and the lower spine were measured. The lumbar force, pubic force and rib deflection were also evaluated. These results were compared to the results obtained with the model of the ES2-re, a side impact dummy, in the same configurations of tests.

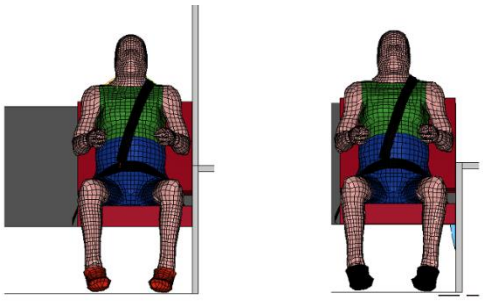

Figure 1 Close wall and arm-rest tests setups

3. Results and Discussion

For the close wall test, the kinematics of HUMOS2 AERO model was divided into several stages: at first, just the left arm was compressed by the wall. Then the pelvis and the left part of the torso were stopped by the wall, and the head hit the wall. The left arm went forward and the left clavicle was broken. HUMOS2 AERO then rebounded. The kinematics of the ES2-re model was similar, but the fractures could not be observed.

The acceleration curves were similar for the ES2-re and HUMOS2 models (Fig 2).

However differences were observed concerning the measure of rib deflection: the lower ribs of the HUMOS 2 AERO model were more loaded than the upper ribs, which was not observed with the ES2-re model. This difference was explained by the shape of the ribcage, which had an influence on the kinematics of the model. In the case of the ES2-re model, which had a cylindrical shape, the load was distributed equally along the ribcage. On the contrary, the ribcage of HUMOS2 AERO had a conical shape: the lower ribs were more loaded than the upper ribs.

The pubic force measured with HUMOS2 AERO model was lower than the pubic force in the ES2-re model. This was due to the modeling of the pelvis area : the loadcell block, the sacrum block and the pelvis bolt were modeled as rigid bodies in the ES2-re model. In HUMOS2 AERO, only the femoral heads were modeled as rigid bodies. As a consequence, the deformation of the pelvis of HUMOS2 AERO was more important and pubic force was lower.

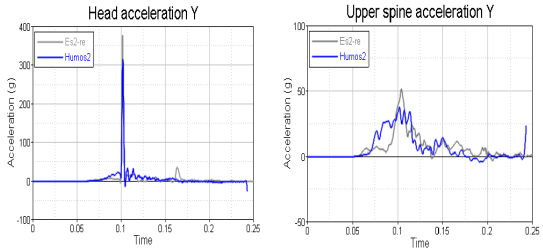

Figure 2 Comparison of accelerations between HUMOS2 AERO (blue) and ES2-re (grey) model

For the armrest test, the kinematics between the two models were different. For the HUMOS 2 AERO model, the left leg and the pelvis were stopped by the arm-rest while the torso kept on going sideward. The rotation of the pelvis around the armrest was observed, which was possible because HUMOS 2 spine was less rigid than ES2-re (Fig 3). The spine was broken at the junction between the lumbar and thoracic vertebrae.

The accelerations were different between the HUMOS2 AERO and the ES2-re models, especially in the upper part of the model. This was explained by the kinematics differences.

Fractures of the clavicle and the lower ribs in the HUMOS2 AERO were also observed.

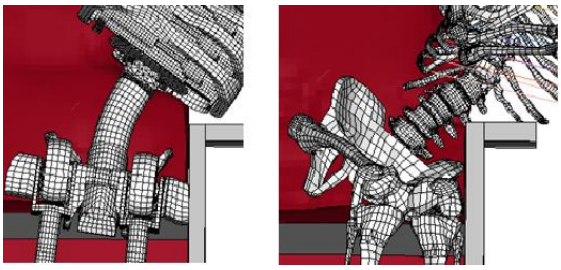

Figure 3 ES2-re model and HUMOS2 AERO in armrest configuration

4. Conclusions

In side-facing tests, the HUMOS 2 AERO model has enabled to predict injuries which were not observed with the ES2-re model, due to the stiffness of the Anthropomorphic Test Device (ATD). Some results (accelerations, force) were also different between the two models, which indicates the interest of using finite element models representing more accurately the human body.

A limit of this study was the lack of comparison with PMHS (post mortem human surrogates) experimental results. Future work should focus on conducting side facing tests using PMHS in order to validate the results obtained with the HUMOS2 AERO model.

Acknowledgments

Martin Poupeney, Samuel Bidal and Jean Michel Terrier from Altair Development France, Antony, France

Gerardo Olivares and Luis Gomez from National Institute for Aviation Research (NIAR), Wichita Kansas, USA

The Civil Aerospace Medical Institute (CAMI)

References

AC 20-146. 2003. Methodology for Dynamic Seat Certification by Analysis for use in Parts 23,25,27 and 29 Airplanes an Rotorcrafts, Federal Aviaiton Adminstration

DeWeese RL, Moorcroft DM, Green T, Philippens MMGM. 2007. Assessment of injury potential in aircraft side-facing seats using the ES-2 anthropomorphic test dummy, Federal Aviation Administration

Njilie F, Kerrien J, Terrier JM, Olivares G, Gomez L. 2012. Human Body Model Evaluation for Aerospace crashworthiness applications, Aerospace Structural Impact Dynamics International Conference – Wichita

Philippens MMGM, Forbes PA, Wismans JSHM, DeWeese R, Moorcroft D. 2011. Neck injury criteria for side-facing aircraft seats, Federal Aviation Administration

Finite element study of cervical spinal dislocation with spinal cord injury preliminary results

L. Fradet[1,2 (*)], P.J. Arnoux[1] and V. Callot [2]

[1] *Laboratoire de Biomécanique Appliquée, Aix Marseille Université, IFSTTAR-, Faculté de Médecine secteur Nord, Boulevard Pierre Dramard, F-13916, Marseille, Cedex 20, France.*

[2] *Aix-Marseille Université, CNRS, CRMBM UMR 7339, 13385, Marseille, France.*

Keywords*:* finite element modeling; cervical spine; dislocation.

1. Introduction (times new roman 12 bold)

In 2005, 1.6 million spinal injuries were reported in the United-States (Martin et al.), 20.8% of which are cervical injuries (Leucht et al.). In particular, spinal cord injuries without radiologic abnormality (SCIWORA) are frequent, and notably difficult to diagnose, due to the absence of hard tissue fracture. Moreover, there are no studies in the literature presenting quantitative data and thresholds concerning cervical dislocations. In this study, a biomechanical analysis of cervical spine dislocation, with and without bone injury is proposed. It will allow the identification of biomechanical risk factors for cervical spine dislocation.

2. Methods

A finite element model of the C5-C6 segment was developed, based on the existing thoracolumbar model Spine Model for Safety and Surgery. Vertebras, intervertebral discs, ligaments, and spinal nervous system were included in this model. Material properties were calibrated on dynamic in vitro experimental data. Element size between 0.5 and 2mm allowed an accurate representation of the geometry. The C6 vertebra was fixed in all directions, and an imposed postero-anterior velocity of $2m.s^{-1}$ was applied to C5. Vertebras were considered as rigid bodies. Three configurations were reproduced. In the first, axial rotation of C5 was allowed, in order to reproduce SCIWORA with a rotation component. In the second, axial rotation of C5 was blocked, in order to reproduce SCIWORA without rotation. In the third, the C5 vertebra was not considered as a rigid body, in order to reproduce a cervical dislocation with fracture of the facets. Injury kinematics was observed. Resulting forces and moments on C6, internal energy, and stress field were measured.

3. Results and Discussion

The analysis of the injury kinematics showed that dislocation without fracture resulted in a contusion of the spinal cord at C5 level, and a traction of the spinal cord at C6 level. Dislocation with fracture showed a contusion at C5 level, but no traction at the lower level. The highest spinal cord traction was observed for SCIWORA with rotation (Figure 1). Analysis of stress field in the spinal cord confirmed this result, and showed higher stresses in the white matter at C6 level for SCIWORA. The highest stresses were observed for SCIWORA without rotation.

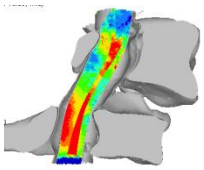

Figure 1 Stress field in the spinal cord. Transverse section. SCIWORA with rotation.

Maximum forces were anteroposterior reaction forces, and were 416, 405, and 179N for SCIWORA without rupture, with rupture and dislocation with facet fracture, respectively. Internal energy at tissue damage was the lowest for dislocation with facet fracture.

4. Conclusions

In this study, biomechanics of cervical spine dislocation was quantified. Also, rotation of superior vertebra, and facet fracture caused by poor bone quality were identified as risk factors.

Acknowledgments

This work was funded by the "Chaire de Neurotrauma de Marseille"

References

Martin, B.I., Deyo, R.A., 2005, Expenditures and health status among adults with back and neck problems, JAMA, 299(6):656-64

Leucht P. et al., 2009, Epidemiology of traumatic spine fractures, Injury, 40(2): 166-172.

***Corresponding author. Email: fradet.leo@gmail.com**

Correcting soft tissue artefact through multi body-optimization: Proposition of an anatomical upper limb kinematic model

A.Naaim†‡, A. El Habachi‡, F.Moissenet†, R.Dumas‡, and L. Chèze*‡

† CNRFR-Rehazenter, 1 rue André Vésale, L-2647 Luxembourg, Luxembourg

‡ Université de Lyon, F-69622, Lyon; IFSTTAR, LBMC, UMR_T9406; Université Lyon 1, France

Keywords*:* upper limb; kinematic model; soft tissue artefacts; multi-body optimization.

1. Introduction

Soft tissue artefact (STA) limits importantly motion capture analysis for upper limb and particularly for the scapula. Different compensation methods, such as the multi-body optimization (MBO) (Duprey et al., 2010), have been proposed. Using MBO, the limb is described as a kinematic chain composed of rigid segments linked by joints. Its kinematics is then optimized in order to fit the segments position by minimising the distance between model-determined and measured marker trajectories under rigid body and kinematic constraints. The aim of this study was to develop a kinematic upper limb model and to compare the effect of the different joint models on the kinematics obtained by MBO on a reach and grasp task.

2. Methods

The upper limb model was composed of six rigid segments (i.e., thorax, scapula, humerus, radius, ulna and hand) linked by seven joints with various constraints. The clavicle was considered as a kinematic constraint and modelled as a constant length between the stenoclavicular and the acromiocalvicular joints. The scapulothoracic joint (ST) was considered as a contact between one (i.e., the middle of the inferior (IM) and superior (SM) scapula contact points (Garner and Pandy, 1999)) or two (i.e., IM and SM) points of the scapula and an ellipsoid modelling the thorax. The glenohumeral joint was modelled as a constant length between the humerus head and the scapula glenoid centers. For the forearm, the Pennestri's model was used in order to respect the anatomy (Pennestrì et al. 2007). This model is composed of three joints: humeroulnar (hinge joint), humeroradial (spherical joint) and radioulnar (linear guide). Finally, the wrist was modelled as a universal joint. The reach and grasp task was recorded using a 100Hz optoelectronic tracking system (Qualysis AB, Gothenburg, Sweden). Markers set, axes' definitions and kinematic calculations were performed following ISB recommendations (Wu et al. 2005).

3. Results and Discussion

The movement of the scapula seems of reduced amplitude without using MBO as it can be seen on Figure 1. The scapula kinematics is significantly changed by MBO with different modifications depending on the scapulothoracic joint model. This illustrates the MBO's effect, where the knowledge of the position of markers all along the chain, can help to constrain the movement of the scapula and can, hopefully, improve kinematics.

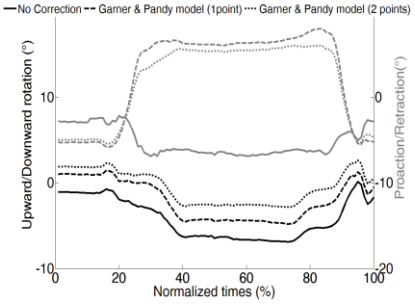

Figure 1 Scapula Up/Downward (black) and Pro/Retraction (grey) kinematics as function of the ST model.

The MBO's effect on the forearm kinematics seems less important on the flexion than on the rotation. The kinematic pattern is similar with only a difference of 10° for the radius rotation and of about 5° at maximum amplitude for radius flexion.

4. Conclusions

For a reach and grasp task, the results seem more promising for the scapula than the forearm. Although, modifications can be small for some movements, the kinematics is effectively modified by MBO. It highlights the need for validations to be able to select the appropriate model in order to correct STA.

References

Duprey, S., Cheze, L., & Dumas, R. 2010. Influence of joint constraints on lower limb kinematics estimation from skin markers using global optimisation. Journal of Biomechanics, 43(14), 2858–62.

Garner, B.A., Pandy, M.G., 1999. A Kinematic Model of the Upper Limb Based on the Visible Human Project (VHP) Image Dataset. Computer methods in biomechanics and biomedical engineering 2, 107-124.

Pennestrì, E., Stefanelli, R., Valentini, P. P., & Vita, L. 2007. Virtual musculo-skeletal model for the biomechanical analysis of the upper limb. Journal of Biomechanics, 40(6), 1350–61

Wu, G., van der Helm, F. C. T., Veeger, H. E. J., Makhsous, M., Van Roy, P., Anglin, C., … Buchholz, B. 2005. ISB recommendation on definitions of joint coordinate systems of various joints for the reporting of human joint motion—Part II: shoulder, elbow, wrist and hand. Journal of Biomechanics, 38(5), 981–992.

***Corresponding author. Email : laurence.cheze@univ-lyon1.fr**

A Meta-Analysis on Biological Variation in Simulations: Importance and Current Modeling Practices.

M. Julias, D. Robertson, and D. Cook

Engineering Division
New York University Abu Dhabi
Abu Dhabi, United Arab Emirates

Keywords*:* Modeling, Simulation, Biological Variation, Finite Element, Averaging

1. Introduction

Significant levels of variability are present in all aspects of human biology, including dimensions and material properties [1,2], stature [3,4], function [5,6], and pathological conditions [7]. However, it is unclear how such variability should be incorporated into biomechanical models.

In the past 10-20 years, several engineering fields have shifted from a deterministic engineering design methodology to a more sophisticated approach which considers the effects of random variation. Biological modeling as a field has not yet undergone a transition from a deterministic to a statistical paradigm. However, such a transition will likely be needed if biomechanical models are to continue to increase in accuracy and relevance. The purpose of this study was to assess the current modeling practices used in the field of and to raise awareness of the importance of biological variability.

2. Methods

A meta-analysis was performed based on research articles published in Journal of Biomechanics in the year 2011. Of the 354 total research articles, 158 articles involved computational modeling to some degree. 60 of these articles were randomly selected and reviewed thoroughly. Descriptive data about model creation and simulation from each manuscript were recorded in a comprehensive database.

3. Results and Discussion

The reviewed articles utilized a total of 1941 distinct model parameters. Only 8 parameters (0.4%) were described in terms of biological variation. Approximately half of all studies utilized medical images as a basis for model geometry and half of those studies utilized multiple samples in the study design. Thus approximately 25% of all studies incorporated some form of biological variability in this way. Histograms of the total number of parameters varied are given in Figure 1.
Nearly every study constructed biomechanical models using average input parameters that had been collected from a number of different individual specimens. The underlying assumption is that the combination of average input parameters to the model will produce average or near average behaviour that can be generalized.

The standard approach in the simulation of many biological systems has become to apply average model inputs and run a limited number of simulations. The application of average inputs to a nonlinear system does not produce average results, and can even produce nonphysical results. An example is shown in Figure 2 which displays the stress-stretch response of several medial-collateral ligaments (MCL) examined in a published peer reviewed study [8]. The grey curves represent the individual responses of the ligaments analyzed while the dotted red curve indicates the response created by applying average constitutive coefficients of the individual ligaments to the constitutive model. The average approach does not produce average behaviour, and actually produces a response which is nonphysical. The occurrence of averaging failure in current biomechanical research is not clear yet we fear that it may be quite pervasive.

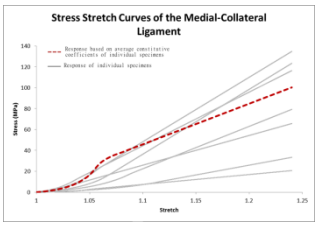

5. Conclusions

Many biological simulations appear to place little emphasis on biological variability. This seems to have led to a situation in which the influence of biological variability is not present in our current literature. In many discussions with our fellow researchers, we have yet to meet an individual who does not agree with the perspective that biological parameters should be considered as random variables. However, this seemingly obvious and important perspective is rarely addressed in the current biomechanics literature.

We recommend the biomechanics community give additional consideration to the issue of biological variation in future studies, and particularly in future conferences. The inclusion of biological variability will lead to studies which produce more reliable results and improve the quality of future research.

***Corresponding author. Email: douglascook@nyu.edu**

References

[1] van Geemen et al. Variation in tissue outcome of ovine and human engineered heart valve constructs: relevance for tissue engineering. Regen Med. Jan;7(1):59-70. 2012.

[2] Yu et al. Variation of certain mechanical properties of human compact bone tissue with age. Polymer Mechanics 10(5), 1974.

[3] Daubes, G. Variations in human stature. Popular Science Monthly. Vol. 31, 1887.

[4] Visscher, P. Sizing up human height variation, Nature Genetics Vol.40, p.489-90. 2008

[5] Tahmoush, D. Modeled gait variations in human micro-doppler. 11th International Radar Symposium, June 16-18, 2010

[6] Brutsaert, T., and Parra, E., Explaining variation in human athletic performance Respiratory. Physiology & Neurobiology Vol. 151, p.109–123 2006

[7] Drumm et al., Genetic variation and clinical heterogeneity in cystic fibrosis. Annu. Rev. Pathol. Mech. Dis. Vol. 7 p.267-282

[8] Quapp et al. Material characterization of human medial collateral ligament. J. Biomechanical Engineering Vol. 120, 6, p.757-763 19

***Corresponding douglascook@nyu.edu**

From spinal cord MRI to a realistic FE model of the spinal cord

Manuel Taso [1,2,3,5], Léo Fradet [1,5], Arnaud Le Troter [2,3], Michael Sdika [4], Jean-Philippe Ranjeva [2,3,5], Pierre-Jean Arnoux [1,5], Virginie Callot [2,3,5]

[1] LBA UMR_T 24, Aix-Marseille Université, IFSTTAR, Marseille, France. [2] CRMBM UMR 7339, Aix-Marseille Université, CNRS, Marseille France. [3] CEMEREM, AP-HM, Pôle d'Imagerie Médicale, Marseille, France. [4] CREATIS UMR 5220 U1044, Université de Lyon, CNRS, Inserm, INSA Lyon, Lyon, France. [5] Laboratoire International Associé en Biomécanique des Traumatismes et Pathologies du Rachis (LIA BSIP)

Spinal cord injury, may it be from traumatic or chronic origin, can lead to severe neurological deficits. Therefore, an accurate characterization of such injuries is of great clinical interest in the management of spinal cord alterations.

Numerical simulation thanks to finite element modeling can provide tools for investigating the mechanical causes leading to morphological and functional alterations. However, the spinal cord presents a complex geometry, with different tissues (presenting different mechanical properties) that needs to be thoroughly taken into account when building FEM of the spinal cord for simulation purposes.

On one hand, the current FEMs of the spinal cord are based either on generic data (a cylinder without differentiation between SC tissues)[1] or post-mortem data (on a single-subject)[2], therefore lacking of both geometrical and biological fidelity and representativity. On another hand, Magnetic Resonance Imaging (MRI) of the spinal cord can provide exquisite details of the SC morphology.

Therefore, the aim of this work was to build a spinal cord atlas[3] (providing a representative average of the SC) of young healthy volunteers, based on high-resolution axial T2* weighted MRI acquisitions, and to use it as geometrical source for providing a realistic *in vivo* SC component inserted into an already existing 3D FEM of the spine (SM2S – Spine Model for Safety and Surgery)[4] developed at the LBA and Montreal (Ecole Polytechnique de Montreal and Ecole de Technologie Supérieure).

To do so, MRI acquisitions were performed at 3T on 20 young volunteers from C1 to T12, providing an entire coverage of the spinal cord. After manual delineation of the SC structures, a semi-automated processing pipeline was developed for the atlas construction. Its representativity of the considered population was assessed. Afterwards, the atlas was positioned into the spine of the SM2S model and meshed into a 3D finite element model.

Applications of this work include FEM analysis of SC trauma or of chronic pathologies such as cervical spondylotic myelopathy (CSM). It is a first step towards more accurate and representative numerical simulation of SC behavior under different loading conditions, but also a first step towards personalized FEM of the SC[5] by using geometrical information derived from MRI as input for FE models.

References: [1] Greaves et al., Ann Biomed Eng n°36, p. 396-405, 2008
[2] Kato et al., J Neurosurg Spine n°8, p. 436-441, 2008.
[3] Taso et al., Magn Reson Mater Phy DOI 10.1007/s10334-013-0403-6, 2013
[4] Wagnac et al., J Biomech Eng n°133, p. 101007, 2011
[5] Lalonde et al., IEEE TBME n°60, p. 2014-2021, 2013

Two-Dimensional Digital Image Correlation (DIC) Efficacy Assessment for Strain Measurement on Bone Surface.

Rafal Perz[1*], Michal Kowalik[1], Jacek Toczyski[3], Marcin Obszański[1],
Jakub Jaroszewicz[2], Krzysztof J. Kurzydlowski[2], Marek Matyjewski[1]

[1 1]*Warsaw University of Technology: Institute of Aeronautics and Applied Mechanics*

[2]*Warsaw University of Technology: Faculty of Materials Engineering*

[3]*University of Virginia: Center for Applied Biomechanics*

Keywords*:* DIC, bone, strains, injury biomechanics

1. Introduction

Bone strain measurements are very common for contemporary biomechanical experiments [1]. Many studies have evaluated the digital image correlation (DIC) method as an effective tool for material deformation measurement in classical experimental mechanics [2], but the method efficacy for bone surface has not been yet explored and quantified. The DIC method is much more versatile than the strain gauges: its active area is only limited by the cameras field of view and it can be used on rugged areas even on micro- and nano-scale. Also DIC expenses are imperceptible comparing to strain gauges.

2. Methods

Figure 1 Example of the sample used

This study sought to evaluate the efficacy and application of the 2D DIC for the bone, through the comparison to the strain gauges method in axial loading test with the porcine bone tissue. A set of 6 samples of porcine metacarpals from rear forefeet was prepared for the purpose of experiment. Each bone has been equipped with three strain gauges and painted with the dot pattern. Additionally, to locate the exact position of strain gauges all the bones were imaged using micro computed tomography (µCT). The experiment was performed using a servo-hydraulic material testing machine with the actuator velocity of 0.5 mm/sec. All the test runs were video recorded (105mm f/2.8 lens, 30fps) to capture the bone surface at the position of each strain gauge. Data was analyzed for the strains, force and displacement. The strain gauges and 2D DIC results were compared to each other and the dispersion was estimated.

3. Results and Discussion

The range of the observed peak strains varied from 0.5 to 3.5 mm/m. Trends observed for the DIC accuracy on bone surface are consistent with the trends observed for other materials. The average difference between strain gauges readings for this dataset was estimated not to excess 5%.

Sample No.	G4A	G4B	G4C	G5A	G5B
Accuracy	2.4%	1.2%	3.5%	4.6%	1.3%

Sample No.	G5C	G6A	G6B	G6C	**Average**
Accuracy	3.7%	3.2%	4.8%	4.9%	**3.3%**

Table 1 Strain gauge vs. DIC methods dispersion for samples G4, G5, G6 and the total average

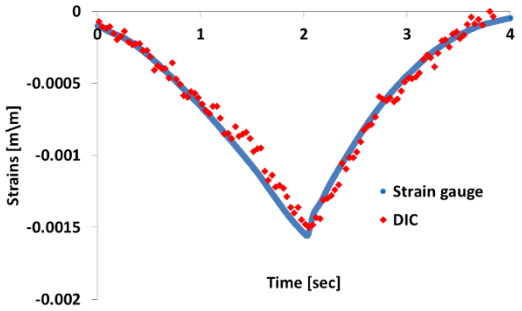

Figure 2 Strains dispersion example for the sample G4B.

4. Conclusions

Obtained data provides insight about the DIC efficacy for the biomechanical experiments. This study shows that the application of the DIC is not limited only to the classic materials but also works very good for the bone tissue with all the benefits of this method.

References

[1] Dongsheng Zhang et al., 2004, Applications of DIC to biological tissues. J. Biomed. Opt. 9(4)

[2] Bing Pan et al., 2009, 2D digital image correlation for in-plane displacement and strain measurement: a review. Meas. Sci. &Techn., vol.

*Corresponding author. Email: rperz@meil.pw.edu.pl

Global and local personalization of a complicated human body FE model.

M.Pedzisz, T.Dziewonski
mpedzisz@meil.pw.edu.pl, tomekn@meil.pw.edu.pl

Warsaw University of Technology, Institute of Aeronautics and Applied Mechanics

Keywords*:* scaling; kriging; personalization; thorax; THOMO;

1. Introduction

Development of human body FE models for injury prediction in car crash conditions is an important subject in recent impact biomechanics. New models, representing medium 50th percentile male and small female, are presented to the world. Regardless of the complexity, all of them need to be verified with respect to the experimental data derived usually from cadaver tests. However, it is a challenge due to anthropometric variety of human body, even for the same group of subjects, their size and gender, and limited validation test data. Therefore, model's personalization is required in order to use available data and as a result improve standard model response.

2. Methods

The dual kriging interpolation was used as a tool for geometry deformation. The existing model was equipped with a set of control points (CPs), carefully selected on a external surface of the body, as well as on internal parts.

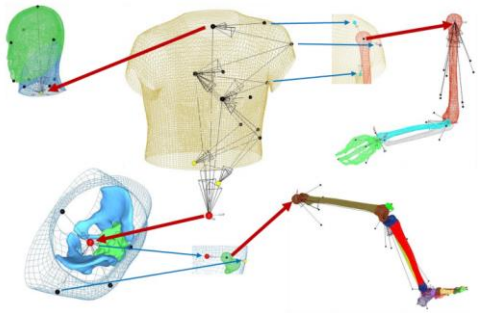

Figure 1 : Dependencies between control points.

The external CPs locations were connected with selected anthropometry measurements taken on the cadavers. While, the internal ones corresponded mainly to the bony parts of the thorax, i.e. ribs, spine, sternum. They were also placed in joints of lower and upper extremities. Additionally, some dependencies between CPs were specified to allow their relative displacements. Up to 750 CPs were defined for the whole model with around 140 needed for controlling global deformation of the geometry.

The prepared methodology is a stepwise approach and requires access to the geometry of the ribcage derived from e.g. CT scans, as well as other information about modelled subject, e.g. anthropometry data, mCT scans of selected bones. Therefore during the study, besides mesh deformation, some other model parameters were personalized. Ribs cortical bone thickness was modified based on available data. The full body mass was personalized as well. It was an effect of reference model selection with simplified leg.

3. Results and Discussion

The aim of the research was to develop a methodology which enables generation of personalized full body human model basing on existing FE model, and allows the direct use of experimental test data for reference model response improvement. A promising result was obtained for six subjects, which was confirmed not only by plain visual comparison, but also with the use of multidirectional measurement procedure developed at University of Valenciennes (UVHC) for cadaver's ribcage assessment. FE mesh quality of personalized models after kriging process was analysed. It did not show any significant difference with respect to the reference geometry.

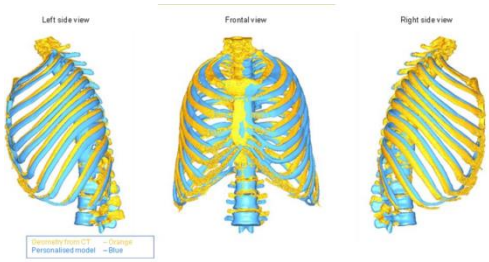

Figure 2 : Comparison of the personalized model geometry (blue) with the reference cadaver CT scan (orange).

Acknowledgments

This study was performed within THOMO project founded by EC in 7th Frame Programme. It was also supported by the National Science Centre (Poland) grant no. DEC-2012/07/B/ST8/03993.

Towards splenic modelling: what is the impact of spleen anatomy on injury severity in blunt splenic trauma?

Anne-Sophie Studer[1,2,4], Thierry Bege [1,2,4],Stéphanie Coze[1,3], Cyril Kahn [1,4], Anderson Loundou[5], Marc Léone[1,6], Kathia Chaumoitre[1,3], Stéphane V. Berdah[1,2,4], Christian Brunet[1,2,4].

[1]*Aix-Marseille University, LBA UMR 24, 13916 Marseille, France*
[2]*AP-HM, North Hospital, Department of digestive surgery, Marseille, France.*
[3] AP-HM, North Hospital, Department of Imaging and Interventional Radiology, Marseille, France.
[4]*IFSTTAR, LBA UMR 24, 13916 Marseille, France* AP-HM, North Hospital, Department of General and Digestive Surgery, Marseille, France
[5] Department of Clinical Research, Unit Help Methodology in Clinical Research, Laboratory of Public Health, Timone, Marseille, France
[6]AP-HM, North Hospital, Department of Anesthesiology and Intensive care, Marseille, France.

Key Words: Human spleen, mechanical characterisation, experimental test, rupture.

1 Introduction

In the field of road safety and numerical simulation of the behaviour of organs in the human body during an accident, it is necessary to carry out bio-faithful experimental tests. Biomechanical properties of tissues represent the main issue of modeling organs. To our knowledge, there is no experimental tests conducted on fresh human spleen. Thus, our study focuses on the structural and biomechanical properties of full human spleen solicited in compression and comparing fresh and cadavers human spleens.

2 Methods

We performed experimental quasi-static compression tests on human full spleen. Fresh tissues are coming from donors during multiorgan retrieval, with the agreement of the French Biomedicine Agency. Then, we compared the data collected from a group of n=8 fresh spleens (group FS) to a group of n=3 human cadavers' spleens embalmed in a Winclker's buffer (group ES). FS group is composed of seven men and one woman spleens of mean age 55 ± 13 years. Before the experimental test, we measured the following splenic morphometric parameters : mass (g), volume (cc), short axis, long axis and splenic thickness to the hilum (mm). To perform the test, we used a hydraulic compression cylinder (MTS, MN, USA), connected to a tri-axis sensor of 15kN, and we applied a compression at a speed rate of 80mm/min, until 60% of compression of initial splenic thickness.
Results are presented as median (min - max) or mean ± standard deviation, and statistical analysis are performed using the Mann-Whitney test.

3 Results and Discussion

In the groups FS and ES, spleens had respectively, a mass' mean of 153 ± 72 and 142 ± 92.2 g, a volume's mean of 163.5 ± 73.4 and 140.7 ± 92.5 cc and a mean of thickness of 32 ± 8 and 35 ± 13 mm. We compared the strength-elongation curves between FS and ES groups which revealed a non-linear behaviour. The median force for which occured the first rupture of the spleen during tests, is 176N (134-424N, FS group) versus 166N (138-228N, ES group). The median of the compression rate, corresponding to the occurrence of the first rupture of the spleen, is 38% (24-56%, FS group) versus 49% (44-54%, ES group). Statistically, the tissue components of the organ in the FS group seemed more resistant to compression stress than in the ES group. Thus, force during the

compression tends to be higher in the group FS, for an equal compression rate.

4. Conclusions

Very few results are available in literature on human fresh spleen to date. And, it emerges differences in results between fresh and embalmed spleen when tested in quasi static compression. This is consistent with data from the literature and this highlights the need to use fresh tissue to be bio-faithful as possible. These preliminary datas will be strengthened by a larger effective in both groups to the same speed rate. This study is part of an investigation to characterise the spleen behaviour in compression for a wide range of speed rate from quasi static to simulated impact. Thus, the biomechanical data that will be extracted, will be used for numerical simulation of the spleen in the human body for traumatology field.

References

1. Boon K. Tay, Jung Kim, and Mandayam A. Srinivasan, *In Vivo* Mechanical Behavior of Intra-abdominal Organs, IEEE Transactions on Biomedical Engineering, VOL. 53, NO. 11, November 2006.

2. J. Stingl, V. Baca, P. Cech, J. Kovanda, H. Kovandova, V. Mandys, J. Rejmontova, B. Sosna, Morphology and some biomechanical properties of human liver and spleen, Surg Radiol Anat (2002) 24: 285–289.

3. Jacob Rosen, Jeffrey D Brown, Smita D, Mika Sinanan, Blake Hannaford, Biomechanical Properties of Abdominal Organs In Vivo and Postmortem Under Compression Loads, Journal of Biomechanical Engineering APRIL 2008, Vol. 130.

4. S. Nicolle, L. Noguer, J.-F. Palierne Shear mechanical properties of the spleen: Experiment and analytical modelling, Journal of the mechanical behavior of biomedical materials 9 (2012) 130–136.

5. Sagar Umale, Caroline Deck, Nicolas Bourdet, Parag Dhumane, Luc Soler, Jacques Marescaux, Remy Willinger, Experimental mechanical characterization of abdominal organs: liver, kidney & spleen, Journal of the mechanical behavior of biomedical materials 17 (2013) 22–33.

***Corresponding author. Email: annesophiestuder@yahoo.fr**

Blunt hepatic trauma: Influence of liver morphology in patients evaluated with volumic CT scan

S. Coze[1] and K. Chaumoitre[1,2 (*)]

[1] *Imaging Department, North Hospital, Marseille, France*

[2] *UMR 7268 CNRS*

Keywords*:* liver trauma, liver morphology, multidectector CT scan, multiplanar reconstructions

1. Introduction

Multidetector computed tomography (MDCT) imaging is a core aspect in the management of liver traumas allowing multiplanar and 3D analysis. The biomechanical forces applied to the liver during a trauma are directly dependent on the anatomy of the organ. We investigated the influence of the liver morphotype on a wide range of blunt liver traumas.

2. Methods

We retrospectively analyzed the demographics, mechanism of trauma and severity of hepatic and concomitant organ injuries in 85 consecutive patients (mean age of 32 years, sex ratio 2M/1W) with blunt hepatic injuries. All of the patients were examined using 64-row MDCT with dual-phase CT. Multiplanar analysis was performed by two readers with specific attention to liver lesions. We defined the liver morphology visualized using MDCT according to diameter (vertical hepatic arrow and antero-posterior diameter). A ventropetal liver (VL) corresponded to a larger antero-posterior diameter, and a dorsopetal liver (DL) corresponded to a larger vertical hepatic arrow. Management and follow-up were also analyzed according to diameter measurements.

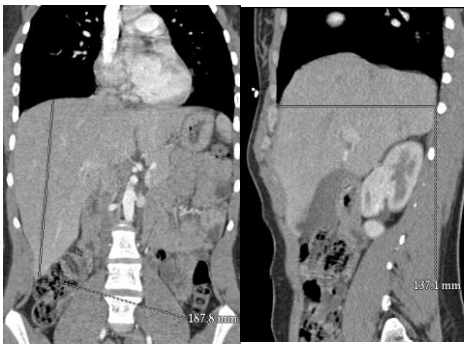

Fig 1: Dorsopetal liver (DL) with maximal development of the right liver. Right liver crosses the ribs

3. Results and Discussion

There were no differences in the trauma circumstances or severity of the trauma between the two groups. The patients in the DL group were significantly younger than the patients in the VL group (mean age of 26.5 and 38.2 years, respectively, p=0.0006). On the initial MDCT, there were no differences between the groups in terms of AAST classification, associated lesions, the number of segments involved, the type of lesion observed (e.g., laceration, contusion or hematoma), or proximity of vascular pedicles. However, there was a significant difference (p=0.03) in the distribution of the lesions. There were statistically more lesions in the right liver in the DL group more lesions in the left liver in the VL group (p<0,05).

	VL liver (n=38)	DL liver (n=47)
Left liver injury	42.1% (n=16)	19.1% (n=9)
Right liver injury	26.3% (n=10)	51.1% (n=24)
Both	31.6% (n=12)	29.8% (n=24)

4. Conclusions

Variations in the morphology of the liver affect the distribution of injury to the liver during blunt trauma. Although this concept has no impact on the clinical assessment or management of patients, evaluating the differences in liver morphology improves the understanding of the mechanical phenomena involved in traumatic injuries.

References

Cheynel N, Serre T, Arnoux PJ, Ortega-Deballon P, Benoit L, Brunet C., 2009, Comparison of the biomechanical behavior of the liver during frontal and lateral deceleration, J Trauma 67:40-4.

***Corresponding author. Email: kathia.chaumoitre@ap-hm.fr**

Influence of car design in typical child pedestrian accident: a parametric study

D. Montoya(*), L.Thollon, S. Berdah, M. Behr

Laboratoire de Biomécanique Appliquée, UMRT24 IFSTTAR/Aix-Marseille Université

Keywords*:* Child, Pedestrian, Parametric, Road safety, Car design

1. Introduction

In 2010, 1210 children under 14 died in road accidents in the USA, among which 256 were pedestrians (IRTAD database). The progress realized on vehicles toward pedestrians mainly focused on the adult. To improve child pedestrian protection and better understand specific injury mechanisms, numerical models are often preferred to post mortem human surrogate tests for obvious ethical reasons. Multi-body (MB) and finite element (FE) are the two most commonly used approaches and both present specific advantages. MB models provide data about kinematics and injury criteria, while FE models provide data on injury mechanisms. The current study explores the possibility to combine both approaches to build a powerful parametric tool able to predict injury assessment in typical child pedestrian accident scenarios previously identified in Literature.

2. Methods

A comprehensive review of the child pedestrian accident was realized based on available Literature data and the IRTAD database. It allowed us to define typical scenarios of accidents, concerning both impact situation and injury distribution.

A parametric analysis software was realized. Several parameters were considered, including vehicle shape and vehicle stiffness. For each scenario and set of parameters, the software first generates a multi-body model of the accident to extract kinematic conditions at the impact. These conditions are used to generate three finite element models, one for each most previously identified injured body region, i.e. head, abdomen and lower limbs. For each iteration, an injury score is established based on recorded injury criteria and injury mechanisms.

3. Results and Discussion

In 2010 in the USA, for road users under 14, the pedestrian accident was the second leading cause of injury and death. The child is mostly struck by light vehicle when crossing the road while running. He is mainly injured at the head, abdomen and lower limbs. The child has a lesion assessment which differs from the adult. Indeed, he is more often slightly wounded in the head but globally less often severely affected.

From the previously described method, we evaluated the influence of vehicle shape parameters on child's head lesions. The results allow us to assess the influence of vehicle front (height bumpers, hood distance, angle hood) on the risk of lesion at the head incurred by the child pedestrian. A statistic study of the results brings out the influence of combination of variables on specific injuries.

The same method should be applied to assess the influence of his same parameters on the abdomen and lower limb.

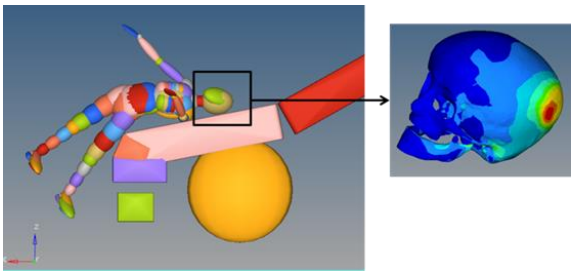

Figure .1 Multibody simulation of the complete accident and Finite Element simulation of the head impact

*Corresponding author : damien.montoya@ifsttar.fr

Scaled model for pedestrian safety

J. Vychytil[1], L. Hynčík[1 (*)], J. Maňas[2] and L. Kovář[2]

[1] *New Technologies – Research Centre, University of West Bohemia, Univerzitní 8, 306 14 Plzeň, Czech Republic*

[2] *MECAS ESI s.r.o., Brojova 16, 326 00 Plzeň*

Keywords*:* virtual; human model; scaling; pedestrian; validation

1. Introduction

The novel approach for development human body model is used to develop VIRTHUMAN, a scalable multi-directional hybrid model for safety.
Previously developed scaling method is applied to develop a pedestrian model according to the PMHS data and the impact response is compared to experimental data by numerical simulation.

2. Methods

A new human body model VIRTHUMAN is developed and fully validated (Vychytil et al. 2014). The model structure is based on rigid bodies connected with joints to ensure global body articulation where the rigid bodies carry so called "superelements" that allow local deformation.
The reference model is developed corresponding to 50% anthropometry is fully scalable based on height, mass and age (Hyncik et al., 2013) using a huge anthropometrical database.
Due to the simple articulation, the model is quickly adaptable to any impact scenario. The pedestrian response according to the PMHS test (Kerrigan et al. 2005) is analysed in the current paper. The model is scaled in order to fit to the PMHS anthropometry and it is set up exactly according to the experimental scenario. The impact simulation was run (see Figure 1) and head velocity and trajectory as well as spinal vertebra and pelvis trajectories relative to the vehicle are monitored.

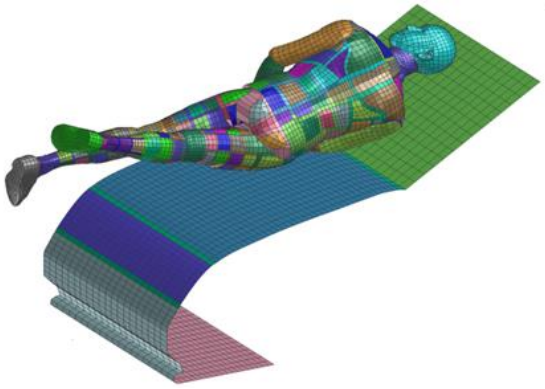

Figure 1 Virtual pedestrian impact.

3. Results and Discussion

The kinematics of the model is satisfactory in terms of displacements as simulated curves are within the corridors with negligible minor overlapping. Kerrigan et al. (2005) performed the pedestrian test also with the Polar-II dummy. The Wrap Around Distance (WAP) and the Time of the Head Strike (THS) are also evaluated and compared in Table 1.

Subject	WAD [mm]	THS [ms]
PMHS	2310*	145*
Polar-II	1947	128
VIRTHUMAN	2295	147

Table 1 WAD and THS values (* Average values by Kerrigan et al., 2005)

4. Conclusions

The model shows very good response comparing to the experimental PMHS test.
The work contributes to the development of virtual human models for design and optimization of safety systems used in various modes of transportation.

Acknowledgments

The work is co-financed by the technology Agency of the Czech Republic within the project TA01031628 "Scalable human models for increasing traffic safety" and within the project SGS-2013-026 "Development of biomechanical models for medicine".

References

Hyncik, L., Cechova, H., Kovar, L., and Blaha, P., 2013, On Scaling Virtual Human Models. SAE Technical Paper 2013-01-0074.

Kerrigan, J.R., Murphy, D.B., Drinkwater, D.C., Kam, et al.., 2005, Kinematic Corridors for PMHS Tested in Full-Scale Pedestrian Impact Tests. 19th ESV Conference, Paper number 05-0394.

Vychytil, J., Manas, J., Cechova, H., Spirk, S. et al., 2014, Scalable Multi-Purpose Virtual Human Model for Future Safety Assessment. SAE Technical Paper 2014-01-0534.

***Corresponding author. Email: hyncik@ntc.zcu.cz**

Assessment methodology of Active Pedestrian Safety Systems: an estimation of safety impact.

H. Hamdane[1,2,3(*)], R. Anderson[2], C. Masson[3], M. Llari[3], T. Serre[1]

[1] *IFSTTAR-LMA, France*

[2] *University of Adelaide, CASR, Australia*

[3] *IFSTTAR-LBA, University of Aix-Marseille, France*

Keywords*:* Pedestrian accident; Active Safety System; accident reconstruction; multi-body simulation

1. Introduction

Devoid of any protection, pedestrians are highly vulnerable to road accidents against a vehicle. To enhance their protection, new safety-based technologies have been introduced in the vehicle market. These on-board systems are developed to prevent crashes from occurring or reduce their severity by reducing the impact speed. Several methods assessing these systems have been presented (e.g. Lindman et al. 2010). This research is focusing on assessing the benefit of Active Pedestrian Safety Systems (APSS's) for pedestrian injury mitigation. Researchers have established a relationship between impact severity and variations in speed impact (Rosén et al., 2010; Anderson et al., 2012). This project is examining the effect of speed reduction on variations in impact conditions.
Outlines of the assessment method are presented here illustrated with one example.

2. Methods

The first step consists of gathering a sample of real vehicle/pedestrian crashes provided by in-depth crash investigation. A considerable level of details is required to reconstruct numerically the pre-crash sequence including trajectories of the vehicle and pedestrian prior to the collision and the eventual obstacles. Each crash is modelled by representing the vehicle and pedestrian involved and the road environment. An APSS is then virtually represented by the parameters of the sensor and actuator.
Once modelling has been set up, all the required components of each sub-model (crash environment, vehicle, pedestrian, and sensor and actuator technology) are implemented through a computational simulation and so interacting in a virtual environment identical to the real world crash scenario. This batch simulation provides a set of data displaying a new impact speed distribution. This distribution is estimated according to the actuation of the emergency braking manoeuvre.
The last step is to estimate change in injury outcome using the HIC. These changes are calculated through the use of multi-body system (MBS) software, MADYMO®. The real accident is firstly simulated in order to obtain the actual risk. Finally, by adding the effect of the emergency braking manoeuvre, the simulation enables to find out if the risk is reduced.

3. Results and Discussion

To show the possibilities of this assessment method, an accident case has been selected.

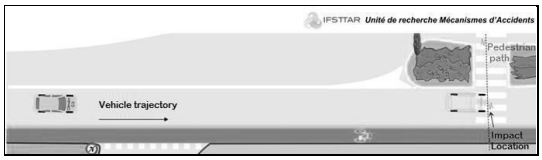

Figure 1 Scheme illustrating the crash scenario

In the original configuration of the crash, the HIC was 1645.6 for an impact speed of 37 km/h. With an APSS fitted in the vehicle, the impact speed is reduced to 8.9 km/h and the pedestrian head doesn't hit any part of the vehicle and hit the ground resulting in a very low HIC value of 28.2.

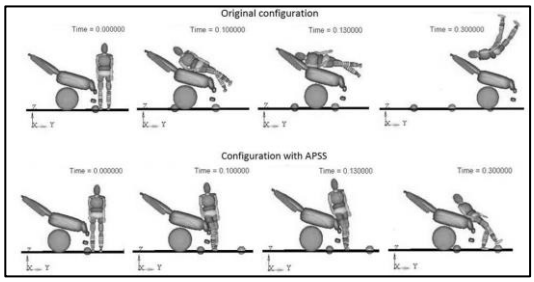

Figure 2 Crash simulation with and without APSS

4. Conclusions

In this research, a formalized assessment methodology has been presented and illustrated with one case to forecast the safety benefits of APSS. This method is based on confronting these systems to real accident configurations through computational simulations. The safety impacts of these systems is then estimated by comparing injury outcome with and without the system enabled for the crash set.

References

Anderson, R.W.G., and al. 2012. Potential benefits of forward collision avoidance technology (CASR106).

Lindman, M., and al. 2010. Benefit estimation model for pedestrian auto brake functionality. Proc. of the 4th Int. Conf. ESAR, Hanover, September 2010.

Rosén, E., and al. 2010. Pedestrian injury mitigation by autonomous braking. Accident Analysis & Prevention (42:6): 1949-1957.

* **H. Hamdane. Email: hedi.hamdane@ifsttar.fr**

Predicting adverse fetal outcomes in road accidents

F. Auriault*[1], L. Thollon[1], J. Peres[1], S. Berdah[1], M. Behr[1]

[1] *Laboratoire de Biomécanique Appliquée, UMRT24 IFSTTAR/Aix-Marseille Université, Marseille, France*

Keywords*:* Injury criteria, Road safety, pregnant woman, fetal outcome

1. Introduction

Road accidents are the leading cause of fetal loss (FL) resulting from trauma. The number of FL resulting from road accidents ranges from 865 to 2795 yearly in the United States according to estimates. To predict adverse fetal outcome with finite element simulations, an injury criterion based on mechanical events at the gravid uterus level during a crash is needed. Several predictors of adverse fetal outcome (major complication or fetal loss) have been proposed in the literature using computational or physical pregnant woman model. The aim of this study is to propose a new predictor of adverse fetal outcome implemented in the PROMIS (PRegnant car Occupant Model for Impact Simulations) model which is a finite element model representative of pregnant woman at 28 weeks of amenorrhea [1]

2. Methods

The PROMIS model has been used to simulate a total of 8 car crash accident conditions. The model includes a gravid uterus with a fetus, a placenta, amniotic fluid and sacral ligaments. Its mechanical response was evaluated and validated against experimental test results [1]. To this study, it has been positionned on a sled including a 3-pt belt, a pretensioner, an airbag and a load limiter.

For each simulation, a corresponding risk of fetal adverse outcome was associated according to the risk curves from the litterature [2].

After each simulation, several predictors at the level of the gravid uterus segment were evaluated, including an original predictor corresponding to the proportion of uteroplacental interface (UPI) reaching a preset strain threshold.

3. Results and Discussion

The 8 car crash configurations were simulated in order to estimate the correlation between each predictor and the fetal adverse outcome associated risk. The typical pregnant woman kinematic during a frontal crash at 50km/h is illustres on figure 1.

A linear regression was performed and the new predictor varied according to the crash configuration associated risk with a correlation value R^2 of 93%.

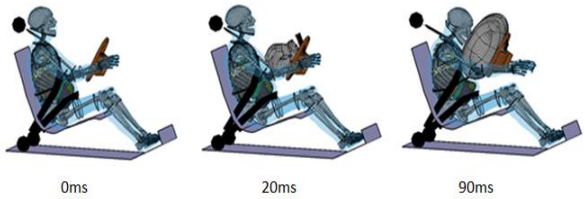

Figure 1:pregnant driver kinematic during a crash

Our results show that a criterion based on a strain distribution rather than on a local peak strain might be more adapted for the correct prediction of an impact consequences. This result is consistent with the fact that the phenomena of placenta abruption is the main fetal mechanism injury resulting from trauma and the risk of fetal loss increase with the proportion of the abruption. This criteria still has at this stage to be considered as qualitative. It will be necessary, before it can be imported in any other finite element model of pregnant woman, to perform a sensitivity analysis to material properties in the UPI area.

References

[1] Auriault, F., Thollon, L., Peres, J., Delotte, J., Kayvantash, K., Brunet, C., and Behr, M., 2014, "Virtual traumatology of pregnant women: The PRegnant car Occupant Model for Impact Simulations (PROMIS)," Journal of Biomechanics.

[2] Klinich, K. D., Flannagan, C. A., Rupp, J. D., Sochor, M., Schneider, L. W., and Pearlman, M. D., 2008, "Fetal outcome in motor-vehicle crashes: effects of crash characteristics and maternal restraint," Am J Obstet Gynecol, 198(4), pp. 450 e451-459.

*Corresponding author : florent.auriault@ifsttar.fr

Suitability of a Multi-Body based Active Human Model for Kinematics and Injuries simulations in an Automatic Emergency Braking Scenario

C. Bastien[1], M. Blundell[1], C. Neal-Sturgess[2], J. Hoffmann[3], A. Diederich[3], R. Van Der Made[4], M. Freisinger[5]

[1] *Coventry University, Priory Street, Coventry CV1 5FB*

[2] *Birmingham University, Department of Mechanical Engineering*

[3] *Toyoda Gosei, Germany*

[4] *TASS, Netherlands*

[5] *OK-Engineering, Germany*

Keywords*:* Active human model, multi-body, pre-braking

1. Introduction

The study assesses the suitability of a multi-body based active human model for the kinematics and injury simulations in an Automatic Emergency Braking Scenario (AEBS). The loadcase investigated combines a typical 1g Autonomous Emergency Braking followed by a secondary 25mph rigid wall impact using a 50th percentile multi-body human body model, which includes full active muscle behaviour.

2. Methods

An initial method of assessing the effect of active safety involving an improved airbag model (Bastien, 2010) and 1'g' pre-brake scenario on an occupant was undertaken (Bastien, 2010) using a passive human model. Further implementations and details were incorporated (Bastien, 2011), included a controlled spine, which allowed the occupant to sit straight and balance its own weight. This study however showed that muscle activity was necessary during the pre-braking phase, hence research involving volunteer physical tests wearing a lap belt was performed under low 'g' sled tests to derive human occupant target motion curves (Bastien, 2012). These were fully validated (Bastien, 2013) and taken as the standard for unbelted pre-braking scenario kinematics and injury simulations.

The paper investigates the effect of the 1'g' pre-braking phase on the unbelted occupant in an emergency stop with no Forward Collision Warning (FCW) considering various steering wheel grips, as well as states of awareness.

3. Results and Discussion

The paper provides a kinematics study of an unbelted bracing human occupant in an AEBS scenario, including various driving postures, state of awareness as well as their respective chest, neck and head injury criteria when the pre-braking phase is followed by a subsequent 25mph rigid wall impact. Occupant's kinematics in pre-braking phase in a 2-hand and 1-hand steering wheel grip are studied, concluding on their respective level of out-of-position.

The paper estimates the suitability of a Multi-Body based Active Human Model for the Kinematics and Injuries simulations as well as the potential of using active human simulation for testing driver assistance safety technologies. The study has not considered the brake dive effects of the vehicle.

4. Conclusions

The paper concludes on the effect of muscle tensioning and on the validity of using active human models for testing driver assistance safety technologies.

References

Bastien C., et al., Correlation of Airbag Fabric Material Mechanical Failure Characteristic for Out of Position Applications , ISMA2010.

Bastien C., et al., Investigation into injuries of Out-of-Position (OoP) posture occupants and their implications in active safety measures, ICRASH 2010.

Bastien C., et al., Investigation Of Pre-Braking On Unbelted Occupant Position And Injuries Using An Active Human Body Model (AHBM), ESV2011.

Bastien C., et al., Influence of human bracing on occupant's neck, head and thorax injuries in emergency braking combined with an FMVSS208 impact scenario, ICRASH 2012.

Bastien C., et al., Safety Assessment Of Autonomous Emergency Braking Systems On Unbelted Occupants Using A Fully Active Human Model, ESV2013.

***Corresponding author. Email: christophe.bastien@coventry.ac.uk**

Outsole material optimization to improve soccer players lower limbs protection

M. Llari[(1)], Y. Godio-Raboutet[(1)], J.L. Guer[(2)], S. Blanchard[(2)], J. Palestri[(2)], L. Thollon[(1)], M. Behr[(1)]

[1] *Aix-Marseille Université, LBA, IFSTTAR, 13916 Marseille, France*

[2] *WIZWEDGE SARL, Bd Camille Flammarion, 13004 Marseille, France*

Keywords*:* outsole; wedge; foot; optimization; biomechanics;

1. Context and Objectives

Soccer players experience an ever greater commitment, as evidenced for example by the constantly increasing number of kilometers traveled during a game. As a consequence, soccer is the sport where players develop the greater number of injuries in proportion to the number of hours of practice, even ahead of rugby according to recent studies (Olsen et al., 2004). To reduce the risk of injury, this study focuses on the shoe protection properties, both in terms of materials used and architecture.

2. Methods

An original outsole architecture, including a removable element (called Wedge) coupled to an arch to support the medium foot and directly molded into the outsole is proposed. Meanwhile, a finite element model of the lower limb has been developed and extensively validated under dynamic loadings, using tests campaigns on cadavers and volunteers.

A database of mechanical properties of 25 foams commonly used in podiatry has also been build, by coupling indentation tests and inverse analysis. Anti-vibration, shock-absorbing and propulsive characteristics of each tested foam were quantified.

The structure and materials of the shoe were then optimized by numerical simulations, using optimization objectives based on biomechanical criteria such as reduced vibrations and stress peaks at the major joints (see Figure 1).

Finally, the optimization results were implemented into a physical prototype of soccer shoe, which was qualitatively evaluated by a professional soccer player.

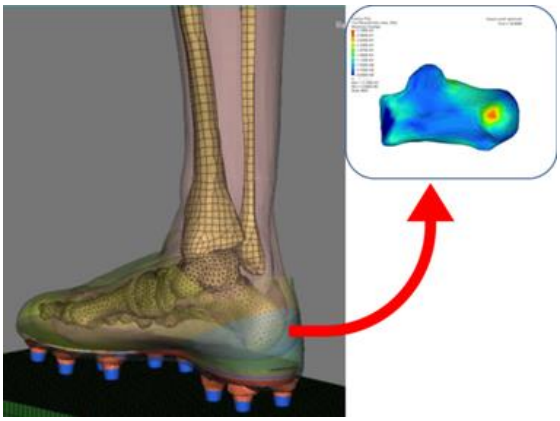

Figure 1. Example of jump landing simulation, and corresponding stress peak recorded on the calcaneum..

4. Results

The characterization of foams revealed a great variety of behaviors. A classification of these foams into three groups (ie anti -shock, propelling and hybrid) could be proposed, with the most efficient materials identified in each of these groups. Optimization made it possible to achieve a combination of structure and associated materials to reduce by up to 80 % vibrations transmitted to the bones and 40 % the recorded peak stresses.

Conclusions

A modification of the outsole structure and materials significantly acts on the biomechanical response of lower limbs (and by extension on the entire human body). A significative improvement of lower limbs exposure to risk of injury can be considered from this type of approach.

References

Olsen L, Scanlan A, MacKay M, Babul S, Reid D, Clark M, Raina P (2004) Strategies for prevention of soccer related injuries: a systematic review. Br J Sports Med. 38(1):89-94.

***Corresponding author. Email: maxime.llari@ifsttar.fr**

Modeling Simulation on Horse-Jockey System

Shuping Li[1,2(*)] ,Yang Yu[2], Jiang Tao [2] and Weiming Zhu[2]

[1] *School of Physical Education, Hubei University, Wuhan, China*

[2] *Center of Motor Control and Evolution, Hubei University, Wuhan, China*

Keywords*:* simulation; spring-mass model; jockey

1. Introduction

Horse race is a movement of the system composed of horse and jockey. Either the jockey's skill level or the style of riding may affect the interaction between jockey and horse (pfau, et al., 2009). For an experienced rider, there was better adaptation to the movement pattern of the horse (Schöllhorn et al., 2006). The purpose of this study was to build a two degree of freedom spring-mass model, simulate the movement horse-jockey system and verify the validity of the simulation.

2. Methods

The two degree freedom spring-mass model was built by adding a one-dimensional spring-mass system of jockey to the one-dimensional spring-mass system of horse (de Cocq, et al., 2013). The connections between horse and jockey as well as horse and ground were both by a linear spring respectively. The differential equations of the two degree of freedom without damping vibration system were analyzed and used to simulate the movement of horse-jockey system.

3. Results and Discussion

In the solutions of differential equation of the two degree of freedom without damping vibration model, the general solution represents the free vibration and the particular solution is for the forced vibration. It indicates that not only the normal movement of horse-jockey system but also the particular time, such as whipping, could be simulated. It shows that the amplitude of the jockey is less than that of horse. The movement pattern of jockey is out of phase to that of horse. The results are similar to the former studies by image analysis of ours (Li, et al., 2009) and inertial analysis of Pfau and his colleagues (pfau, et al., 2009).

4. Conclusions

The two degree of freedom without damping vibration model could be used to simulate the normal movement of horse-jockey system. It is possible to provide insight into those more complex conditions of horse race by further analysis to the model.

References

de Cocq P., Muller M., Clayton H. M., et al., 2013, Modelling biomechanical requirements of a rider for different horse-riding techniques at trot. The Journal of experimental biology. 216(10): 1850-1861.

Li S., Li L., Tao J., et al. , 2009, Jockeys postuer characteristics on the simulation horse. Abstracts of 2009 SimBio-M: 28.

Pfau T., Spence A., Starke S., et al., 2009, Modern riding style improves horse racing times[J]. Science. 325(5938): 289-289.

Schöllhorn W. I., Peham C., Licka T., et al. , 2006, A pattern recognition approach for the quantification of horse and rider interactions. Equine Veterinary Journal, 38(S36): 400-405.

***Corresponding author. Email: spli@hubu.edu.cn, s_p_li@sina.cn**

Parametric study of a snowboarding accident: Implication on helmet standard

N. Bailly[1], C. Masson[1], M. LLari[1], P.J. Arnoux[1]

[1]*Aix Marseille Université, IFSTTAR, LBA UMR_T 24, 13916, Marseille, France*

Keywords*: Multibody simulation, snowboard, head injury, biomechanics*

1. Introduction

Head injury is the primary cause of death and serious disability among snowboarders. In 2002, a very common type of snowboarding fall leading to head trauma was identified by Nakaguchi (Nakaguchi et al. 1999) : he described it as the snowboarder catching the back edge of its snowboard and falling backward. The aim of this work is to develop a multi-body model of snowboarder to provide in depth investigation of this very common snowboarding fall and to gives a new insight on the safety requirement of helmets.

2. Methods

A multibody model(Yang et al. 2000) of pedestrian was adapted to the snowboarder. The stiffness of the snow during the impact with the head was characterised experimentally and implemented in the model. We evaluated our model by comparing the model's kinematics and the acceleration of the head to Scher and al. 's experimental data (Scher, Richards, and Carhart 2006). Finally, hundreds of accident configurations were simulated, in order to investigate the effect of different parameters (initial speed, angle of the slopes, height of the snowboarder…) that may affect the body kinetics of the snowboarder and the head impact. Head velocity, head acceleration, Head Injury Criteria and the impact zone on the head were recorded.

3. Results and Discussion

The model reports good correlation with the experimentation of Scher and al. (Scher, Richards, and Carhart 2006). In most accident configuration the resultant velocity of the head just before the impact is higher than the initial velocity of the snowboarder due to the momentum created during the fall by the height of the snowboarder. When the configuration of the fall involves hard snow, the risk of head injury is very high. This is consistent with the epidemiologic result of Nagakuchi and al (Nakaguchi et al. 1999) and implies the necessity to protect snowboarder's head to prevent injuries from this type of fall. Finally, the normal velocity of the head is most of the time higher than the velocity at which helmets are tested to pass the standard specifications (F08 Committee 2011). Head impacts are also associated with a high tangential velocity which is not taken into account in existing standard specifications (figure 1). Those results question the efficiency of current safety requirements.

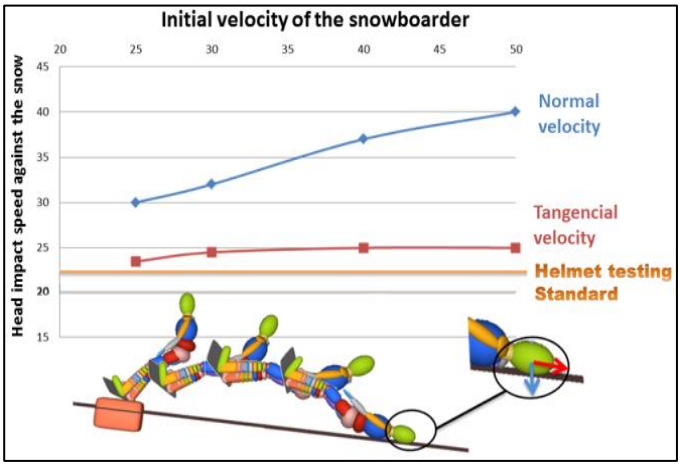

Figure 1: Modelling of the snowboarder fall: analysis of the impact speed

References

F08 Committee. 2011. "Specification for Helmets Used for Recreational Snow Sports". ASTM International. http://enterprise.astm.org/filtrexx40.cgi?+REDLINE_PAGES/F2040.htm.

Nakaguchi, H, T Fujimaki, K Ueki, M Takahashi, H Yoshida, and T Kirino. 1999. "Snowboard Head Injury: Prospective Study in Chino, Nagano, for Two Seasons from 1995 to 1997." *The Journal of Trauma* 46 (6): 1066–69.

Scher, I, D Richards, and M Carhart. 2006. "Head Injury in Snowboarding: Evaluating the Protective Role of Helmets." *Journal of ASTM International* 3 (4): 14203. doi:10.1520/JAI14203.

Yang, J.K., P. Lövsund, C. Cavallero, and J. Bonnoit. 2000. "A Human-Body 3D Mathematical Model for Simulation of Car-Pedestrian Impacts." *Journal of Crash Prevention and Injury Control* 2 (2): 131–49. doi:10.1080/10286580008902559.

***Corresponding author. Email: Nicolas.bailly@ifsttar.fr**

A finite element study of the effects of distraction osteogenesis on the temporomandibular joint

C. Savoldelli[1,2] , P.-O. Bouchard[1] , Y. Tillier[1 (*)]

[1] *MINES ParisTech, CEMEF, CNRS UMR 7635, Sophia-antipolis, France*

[2] *Institut Universitaire de la Face et du Cou, Chirurgie maxillo-faciale et stomatologie, Nice, France*

Keywords*:* 3D Finite element model; distraction osteogenesis, temporomandibular joint, maxillofacial surgery

1. Introduction

Stress modifications resulting from mandibular distraction osteogenesis (DOG) surgery can generate anatomical modifications in the temporomandibular joint (TMJ) discs and be at the origin of disc dislocation with degeneration. This may cause severe oral and facial pain or masticatory dysfunctions. Our study aims at analyzing the stresses distribution during jaw closing cycle, with dental occlusion, in the TMJ using a high-resolution 3D finite element model (Forge®).

2. Methods

Several models of TMJ already exist in literature. But they are often limited to the study of one TMJ and do not take into account the physical asymmetry of the human body. In our model, the geometric data are obtained from a thirty-year-old healthy (asymptomatic joints) and fully dentate male patient. Hard (bones, teeth) and soft (discs, capsules, ligaments) tissues are respectively obtained from CT and MR images. Medical images are processed using a 3D image segmentation software. All tissues are meshed as separate bodies (Figure 1a). The final finite element model consists of 386,092 tetrahedral elements. Material properties are either taken from the literature or characterized using inverse analysis techniques [Odin 2010]. Jaw muscles are represented through force vectors of different directions. Their magnitudes are assigned according to the muscle physiological cross section and scaling factors [Koolstra 1988]. The cartilage layer is taken into account by considering a low friction contact between different bodies. A surgical vertical osteotomy line is simulated on the model by cutting the mesh in the mandibular midline region. A 1 cm expansion procedure is simulated using two forces normal to the cutting planes, applied to both resulting segments of the mandible. This model is representative of a bone-borne expansion device. Von Mises stress distribution in both joint discs before, during and after distraction is analysed during a chewing sequence. The geometry and mesh of the bone callus corresponding to the consolidated bone (after DOG has taken place) are built using a volumic mesher (Figure 1b).

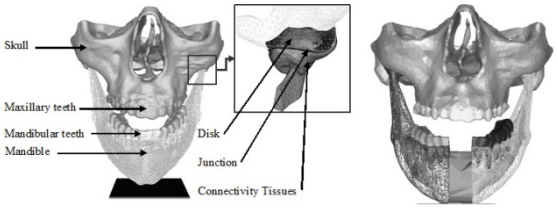

Figure 1: FE model (a) before and (b) after DOG

3. Results and Discussion

As a main result, computed results show that taking into account the morphological asymmetry of the skull induces different stress concentrations on both TMJ discs and in the ascending branches of the condyles. Stress level evolves continuously during jaw movement. Even if maximal stress values are not the same from one side to another, they are observed in the same areas (medial, lateral bands for both discs). The maximum stress intensity reached in the articular discs during chewing is slightly higher after the mandible expansion than before.

4. Conclusions

The present numerical model shows that anatomical changes in TMJ structures are unlikely to predispose to long-term tissue fatigue. Rate and frequency of distraction are probably more important than the amount of distraction itself. This supports the clinical theory that symphyseal distraction generates a low risk of long-term TMJ dysfunction or condylar resorption.

References

Odin, G., Savoldelli, C., Bouchard, P.-O, Tillier, Y., 2010, Determination of Young's modulus of mandibular bone using inverse analysis, Med Eng Phys, 32(6), pp 630-637

Koolstra, J.H., van Eijden, T.M.G.J., Weijs, W.A. , Naeije, M., 1988, A three-dimensional mathematical model of the human masticatory system predicting maximum possible bite forces, J Biomech, 21(7), pp 563-576

***Corresponding author. Email: yannick.tillier@mines-paristech.fr**

Tensile response of muscle-tendon complex using discrete element modeling

A. Roux*†, J. Lecompte†, L-L. Gras†, S. Laporte†, I. Iordanoff‡

† Arts et Métiers ParisTech. LBM. 151 bd de l'hôpital 75013 Paris ;
‡ Arts et Métiers ParisTech. I2M. Esplanade des Arts et Métiers 33405 Talence

Keywords*:* Muscle-tendon complex, Discrete Element Method, pennation angle, hyper-elastic behavior

1. Introduction

Biomechanical models extensively used the finite element methods (FEM) to compute the non-linear behavior of the muscle-tendon complex (MTC) under passive stress. However, FEM appears to be limited when multi-scale structure behavior was of interest. Therefore, the aim of this study was to improve MTC behavior during tensile test using the discrete element method (DEM), focusing on architectural parameters.

2. Material and Methods

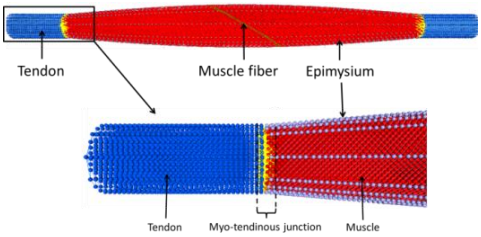

Figure 1: MTC geometry in DEM

The MTC model was developed in DEM (Figure 1) with GranOO software (I2M, France). Mechanical properties of MTC were addressed thanks to literature values (Lieber et al. 2003, Matschke et al. 2013). Stiffness of each element was related to discrete elements' cross-sectional area, initial length of links and corresponding elastic modulus (EM). Fibers were built with spherical discrete elements linked by springs (EM=28.2 MPa). The extra cellular matrix was computed using springs between fibers (EM=100 MPa). Tendon's fibers were built with respect to muscle fibers architecture (EM=800 MPa). The myotendinous junction was represented by multi-links (EM=300 MPa) between tendon and muscle. Force/displacement relationship (F/D) was obtained during a computed tensile test. MTC was fixed on its lower extremity and the upper extremity was subjected to a linear displacement. Thus, stretch-dependent evolutions of muscle volume and pennation angle (PA) were calculated.

3. Results and Discussion

The computed F/D (Figure 2) could be divided into two parts. The first part, when the force was quasi-null, could be attributed to the orientation and alignment of all fibers within the muscle along the linear axis of traction. The second part displayed a classical hyper-elastic behavior (a gap of 2N has been set in order to fit with *in vitro* experimental data of Gras et al. 2012).

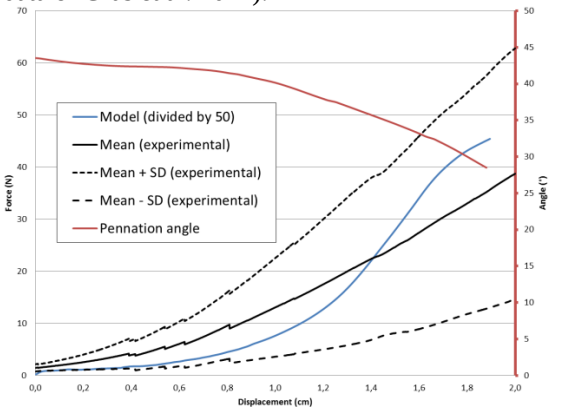

Figure 2: MTC force/displacement curve (blue) and PA/displacement curve (red) with muscle's length=134 mm, tendon's length=20.1 mm, central width=16.1 mm and PA=45°.

Computed F/D shape was in agreement with experimental ones despite a 50 times higher value. This could be attributed to the chosen EM values that were probably not adapted to our model. The decrease of PA during the tensile test was in agreement with *in vivo* assessments. The variation of MTC volume, calculated during the simulation, was less than 1%.

4. Conclusions

The DEM seems to be a promising method to model the hyper-elastic macroscopic response of MTC with simple elastic microscopic elements. The next step will be to improve the model to a hyper-viscoelastic specific issue.

References

Gras L-L., Mitton D., Viot P., Laporte S., 2012 Hyper-elastic properties of the human sternocleidomastoideus muscle in tension. J. Mech. Behav. Biomed. Mater. 15:131-140.

Lieber R.L., Runesson E., Einarsson F., Friden J., 2003 Inferior mechanical properties of spastic muscle bundles due to hypertrophic but compromised extracellular matrix material. Muscle Nerve 28:464–471.

Matschke V., Jones J.G., Lemmey A.B., Maddison P.J., Thom J.M., 2013 Patellar Tendon Properties and Lower Limb Function in Rheumatoid Arthritis and Ankylosing Spondylitis versus Healthy Controls: A Cross-Sectional Study. Sci. World J. 2013:514743.

*Corresponding author. Email: anthony.roux@ensam.eu

Investigation of diffuse axonal injury mechanism and thresholds via the combination of finite element simulation and *in vivo* experiment

L. Ren[1,2], D. Baumgartner[2 (*)], J. Yang[1,3], J. Davidsson[3], and R. Willinger[2]

[1] *State Key Lab of Advanced Design and Manufacturing for Vehicle Body, Hunan University, China*

[2] *ICube Laboratory, University of Strasbourg, France*

[3] *Department of Applied Mechanics, Chalmers University of Technology, Sweden*

Keywords*:* finite element model; diffuse axonal injury; traumatic brain injury; animal experiment; injury mechanism

1. Introduction

The purpose of the current study was to investigate the mechanism and thresholds of diffuse axonal injury (DAI). A series of *in vivo* rat brain injury experiments were reconstructed by using a prior developed and validated rat brain finite element (FE) model. Intracranial mechanical responses of the rat brain and region-specific thresholds for DAI were investigated.

2. Methods

In the *in vivo* rat brain injury experiment, the instant rotational acceleration in sagittal plane was used for the production of DAI in rat brain (Davidsson et al., 2009). The post-trauma rats were sacrificed, and the rat brains were harvested for histological analysis. Coronal 14 μm cryostat sections were cut and incubated with antibodies for β-Amyloid Precursor Protein (β-APP) to detect axonal injury. Axonal injury outcomes were classified into four degrades for frontal, central and occipital region separately, according to the corresponding histological findings (β-APP positive axons) in each region.

The rat brain model used in the current study was composed of 156,656 hexahedral elements and 12,881 shell elements with an average edge size of 0.25 mm (Lamy et al., 2013). And, the rat brain was reorganized into 25 parts, which represented all essential anatomical features of rat brain, such as cingulate cortex, corpus callosum, hippocampus, hypothalamus, cerebellum and brainstem. In simulations, rotational acceleration pulses were applied on the nodes of the skull. Maximum shear strain responses were calculated and compared with injury outcomes.

3. Results and Discussion

Totally, twenty seven cases with classified DAI outcomes were reconstructed, while the magnitude of rotational accelerations ranged from 0.5 Mrad/s^2 to 2.1 Mrad/s^2. As illustrated in Figure 1, highest strain responses were observed in cingulate cortex around simulation time 1.45 ms, followed by strain responses in the central and low area. The high strain responses in the central area were consistent with the distribution of axonal injury in experiments. Moreover, inflammatory responses were observed in cingulate cortex (where highest strain responses were located), but such kind of injury was not investigated in the current study.

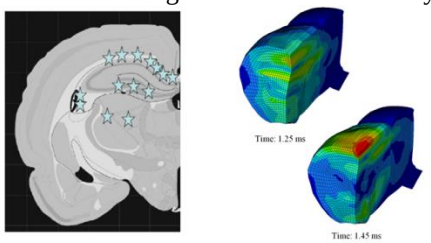

Figure 1 Distribution of β-APP positive axons in coronal plane from impact tests (left) (Davidsson et al., 2009) and contours of maximum shear strain responses from current simulations (right).

Conservative thresholds of the shear strain for axonal injury were 7% in frontal region, 11% in central and occipital region of the rat brain. The difference between axonal injury thresholds in different regions may result from the distribution of thin nerve fibers, and such correlations should be clarified in future studies.

4. Conclusions

Via reconstructions of twenty seven rat impact tests, region-specific threshold for axonal injury in rat brain were investigated. A relative lower threshold for axonal injury was observed in frontal region of the rat brain.

References

Davidsson, J., Angeria, M., and Risling, M., 2009, Injury Threshold for Sagittal Plane Rotational Induced Diffuse Axonal Injuries. In proceedings of IRCOBI Conference 2009, York, UK, pp. 47-55.

Lamy, M., Baumgartner, D., Yoganandan, N., Stemper, B. D., and Willinger, R., 2012, Experimentally Validated Three-Dimensional Finite Element Model of the Rat for Mild Traumatic Brain Injury. Medical & Biological Engineering & Computing, **51**(3), pp. 353-365.

***Corresponding author. Email: daniel.baumgartner@unistra.fr**

Superficial soft tissue modelling in impact loading

F. Lanzl[1,*], K. Zhou[1] and S. Peldschus[1,2]

[1] *University of Munich, institute for legal medicine, Nußbaumstr. 26, 80336 Munich, Germany*
[2] *Hochschulcampus Tuttlingen der Hochschule Furtwangen, Tuttlingen, Germany*

Keywords: finite element, soft tissue, material modelling, high strain rate

1. Introduction

In recent years finite element (FE) models have become a popular method for the assessment of different biomechanical issues. In the field of impact biomechanics they are used to simulate high-rate loading events, such as sporting accidents, car crashes or blunt impacts.[1] The validity of such simulations depends on a proper material description of the involved tissues. But this is challenging, since most biological tissues, like muscle, exhibit a complex material behaviour involving strain rate dependency.[2] So for impact simulations it is important to use a material model capable of representing correct material behaviour even at high strain rates. In this study a rate dependent material description for passive muscle tissue under impact loading was developed and validated against data from volunteer tests.

2. Methods

First a material description for passive muscle behaviour under dynamic compression was developed based on data from the work of Cronin et al., who measured high strain rate compressive behaviour of bovine muscle tissue with a split Hopkinson pressure bar (SHPB) apparatus.[1] The material description was preliminary checked by simulating this SHPB tests. Afterwards volunteer tests were performed by releasing an aluminium impactor upon the upper arm of blindfold persons from different heights (20 cm and 40 cm). The acceleration of the impactor during impact was recorded. Subsequently the material description was validated against the volunteer tests using a FE model of the upper arm based on CT-scan data.

3. Results and Discussion

Figure 1 compares the results of the FE simulation of the SHPB tests with the experimental results of Cronin et al. for strain rates of 1000s^{-1}, 1700s^{-1} and 2300s^{-1}. The simulation curves are generally in good agreement with the experimental ones.

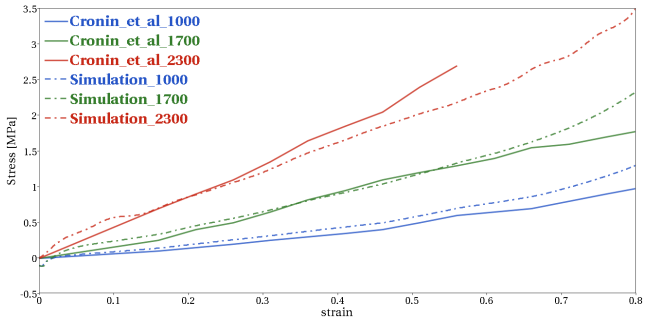

Figure 1 – results of the FE simulation in comparison to experimental results of Cronin et al. [1]

Figure 2 compares the upper and lower corridor of the volunteer tests to the simulation results for a drop height of 20 cm. In principle the simulation results exhibit a good trend towards the experimental behaviour of the muscles. But the developed material model is not capable to reproduce the exact curve shape of the experimental results. Results for a drop height of 40 cm show a similar trend. This might be due to inadequate material modelling of the skin and adipose tissue enclosing the muscle in the FE model. Both tissues are also rate dependent, but no validated rate dependent model for impact loading could be found.[3,4] In addition muscles in the volunteer tests might have not behaved purely passive, even if the volunteers were blindfolded.

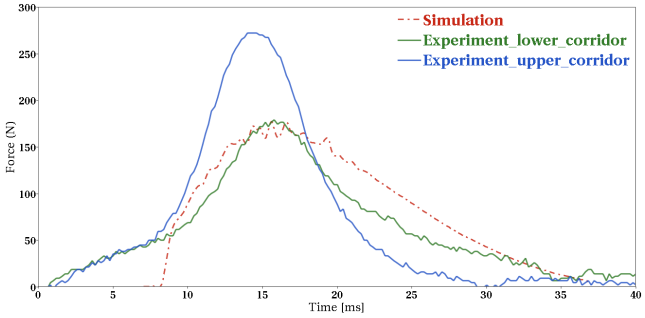

Figure 2 - results of the FE simulation compared to experimental results of the volunteer tests

4. Conclusion

The material description developed in this work can be considered as a good approach to model passive muscle behaviour under high dynamic compression. However, the FE model of the volunteer tests still needs further investigation, especially in terms of material modelling for skin and adipose tissue.

[1] Cronin, D.S., Van Sligtenhorst, C., Brodland, G.W., 2006, High strain-rate compressive properties of bovine muscle tissue determined using a split Hopkinson bar apparatus, Journal of Biomechanics, 39:1852-1858

[2] Van Loocke, M., Lyons, C.G., Simms, C.K., 2006, A validated model of passive muscle in compression, Journal of Biomechanics, 39:2999-3009

[3] Shergold, O.A., Fleck, N.A., Radford, D., 2006, The uniaxial stress versus strain response of pig skin and silicone rubber at low and high strain rates, International Journal of Impact Engineering, 32:1384-1402

[4] Comley, K., Fleck, N., 2012, The compressive response of porcine adipose tissue from low to high strain rate, International Journal of Impact Engineering, 46:1-10

***Corresponding author. Email: felicitas.lanzl@mytum.de**

An upper limb musculoskeletal model using bond graphs for rotorcraft-pilot couplings analysis

Georges Tod, François Malburet, Julien Gomand and Pierre-Jean Barre
georges.tod@ensam.eu, francois.malburet@ensam.eu, julien.gomand@ensam.eu, pierre-jean.barre@unice.fr

Arts et Metiers Paristech, CNRS, LSIS, Aix-en-Provence, France

Keywords*:* musculoskeletal models; multiphysical systems; bond graphs

1. Introduction

Under certain flight conditions, a rotorcraft fuselage motions and vibrations might interact with its pilot voluntary and involuntary actions leading to potentially dangerous dynamic instabilities known as rotorcraft-pilot couplings (RPCs) [1]. A better understanding of this phenomenon could be achieved by being able to reproduce the phenomenon during simulations. Design guidelines could be then obtained at an early stage of development of rotorcrafts improving flight safety for pilots and passengers.
In this work, an upper limb musculoskeletal model using bond graphs is presented. It is then integrated in a larger aeroelastic rotorcraft bond graph model that allows simulating pilot-rotor-fuselage couplings under several flight conditions. Simulations are performed and compared to literature's models and experimental data.

2. Methods

A different approach to analytical derivation of the equations of a dynamical system can be performed using bond graphs. While generating the same mathematical model than traditional methods and based on the same physical principles, it allows a modular approach that might ease the modelling process of large multiphysical systems [2]. Bond graphs describe systems as an interconnection of more elemental subsystems by exchanging energy. This paper contributes to the development of a multiphysical system involving pilot biodynamics, quasi-steady aerodynamics and coupled rotor-fuselage dynamics to study RPCs. In this work, firstly an upper limb skeletal model representing the helicopter's pilot as a multibody system using bond graphs is detailed. Secondly, muscles are added to the skeleton. The muscle models are based on the classic three element Hill model reviewed by Zajac in [3] and implemented using bond graphs in [4].

3. Results and Discussion

The multibody skeletal model is integrated in a rotorcraft model. In order to evaluate its validity, we estimate the pilot's biodynamic feedthrough (BDFT) in the lateral rotorcraft axis: magnitude of the cyclic lever roll angle divided by the fuselage lateral acceleration. Simulation results are compared to Venrooij's experimentally identified transfer functions model during a relax task [5], see Figure 1. The multibody simulation results are obtained by applying a sinusoidal force at a given frequency on the fuselage lateral axis.

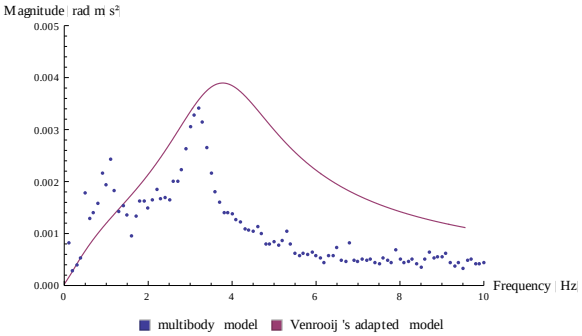

Figure 1. Pilot's biodynamic feedthrough simulation results

A resonant peak is found in both models around 3.5-4Hz. This frequency is of particular interest for rotorcraft dynamicist since the natural frequency of the roll motion of some helicopters is between 2 and 4Hz. The addition of muscles to the skeletal model will also be discussed.

4. Conclusions and future work

This study explores the implementation of musculoskeletal models in bond graphs to better understand RPCs and contribute to their alleviation by analysing simulation results early in the design stage of rotorcrafts.

References

[1] TOD, Georges, MALBURET, Francois, GOMAND, Julien, BARRE, Pierre-Jean et al., An Energetic Approach to Aeroelastic Rotorcraft-Pilot Couplings Analysis, European Rotorcraft Forum, Moscow - Sept 2013
[2] KARNOPP, Dean C., MARGOLIS, Donald L., et ROSENBERG, Ronald C. System Dynamics: Modeling, Simulation, and Control of Mechatronic Systems. Wiley, 2012
[3] ZAJAC, Felix E. Muscle and tendon: properties, models, scaling, and application to biomechanics and motor control. Critical reviews in biomedical engineering, 1988, vol. 17, no 4, p. 359-411.
[4] WOJCIK, Laura A. Modeling of musculoskeletal structure and function using a modular bond graph approach. Journal of the franklin Institute, 2003, vol. 340, no 1, p. 63-76.
[5] VENROOIJ, Joost, PAVEL, Marilena D., MULDER, Max, et al. A practical biodynamic feedthrough model for helicopters. CEAS Aeronautical Journal, 2013, vol. 4, no 4, p. 421-432.